

Solar Cycle in the Heliosphere and Cosmic Rays

Galina A. Bazilevskaya · Edward W. Cliver ·
Gennady A. Kovaltsov · Alan G. Ling · M.A. Shea ·
D.F. Smart · Ilya G. Usoskin

Received: 17 April 2014 / Accepted: 3 August 2014 / Published online: 9 September 2014
© Springer Science+Business Media Dordrecht 2014

Abstract Manifestations of the 11-year solar cycle and longer time-scale variability in the heliosphere and cosmic rays are considered. We briefly review the cyclic variability of such heliospheric parameters as solar wind speed and density and heliospheric magnetic field, open magnetic flux and latitude variations of the heliospheric current sheet. It is discussed whether the local in-situ observation near Earth can represent the global 3D heliospheric

G.A. Bazilevskaya
Lebedev Physics Institute, Russian Academy of Science, Leninsky pr. 53, Moscow, Russia
e-mail: gbaz@rambler.ru

E.W. Cliver
Space Vehicles Directorate, Air Force Research Laboratory, Kirtland AFB, NM 87117, USA

E.W. Cliver
National Solar Observatory, Sunspot, NM 88349, USA
e-mail: ecliver@nso.edu

G.A. Kovaltsov
Ioffe Physical-Technical Institute, St. Petersburg, Russia
e-mail: gen.koval@mail.ru

A.G. Ling
Atmospheric Environmental Research, 3550 Aberdeen Ave., Kirtland AFB, NM 87117, USA
e-mail: aling@aer.com

M.A. Shea · D.F. Smart
SSSRC, 100 Tennyson Av., Nashua, NH 03062, USA

M.A. Shea
e-mail: sssrc@msn.com

D.F. Smart
e-mail: donsmart100@msn.com

I.G. Usoskin (✉)
Sodankylä Geophysical Observatory (Oulu unit) and Dept. Physics, 90014 University of Oulu, Finland
e-mail: ilya.usoskin@oulu.fi

pattern. Variability of cosmic rays near Earth provides an indirect useful tool to study the heliosphere. We discuss details of the heliospheric modulation of galactic cosmic rays, as recorded at and near Earth, and their relation to the heliospheric conditions in the outer heliosphere. On the other hand, solar energetic particles can serve as probes for explosive phenomena on the Sun and conditions in the corona and inner heliosphere. The occurrence of major solar proton events depicts an overall tendency to follow the solar cycle but individual events may appear at different phases of the solar cycle, as defined by various factors. The solar cycle in the heliosphere and cosmic rays depicts a complex pattern which includes different processes and cannot be described by a simple correlation with sunspot number.

Keywords Heliosphere · Cosmic rays · Solar energetic particles · Solar activity

List of Abbreviations

| | |
|-----|---|
| AU | Astronomical unit (the mean Sun-Earth distance, $\approx 1.5 \times 10^{11}$ m) |
| CME | Coronal mass ejection |
| CR | Cosmic rays |
| GLE | Ground-level enhancement of cosmic rays |
| GCR | Galactic cosmic rays |
| HCS | Heliospheric current sheet |
| HMF | Heliospheric magnetic field |
| IC | Ionization chamber |
| MHD | Magnetohydrodynamics |
| NM | Neutron monitor |
| OMF | Open magnetic flux |
| SEP | Solar energetic particles |
| SPE | Solar proton events |
| SSN | Sunspot number |

1 Introduction

The heliosphere is a cavity in the interstellar plasma controlled by the solar wind continuously emitted by the Sun and by heliospheric magnetic field (HMF) ultimately produced by the solar dynamo (see, e.g. recent reviews by (Owens and Forsyth 2013; Balogh and Erdős 2013). The exact size of the heliosphere may vary in the course of solar cycle (e.g., Pogorelov et al. 2013, and references therein). It consists of three main regions separated by clear boundaries.

- The termination shock bounds the region of supersonic solar wind with frozen-in HMF. This is an approximately spherical region with a radius of about 90 AU. The heliosphere inside the termination shock does not “know” (in the MHD sense) about the presence of anything outside. The termination shock was discovered by Voyager-1 at the distance of 94 AU in 2004, and by Voyager-2 at 84 AU in 2007 (Stone et al. 2005, 2008).
- The region beyond the termination shock is still filled by the solar wind and HMF, but those are distorted by the presence of the interstellar wind. This region is bounded by the heliopause which is non-axisymmetric. Its size is about 122 AU in the nose direction, as discovered by Voyager-1 in 2012 (Stone et al. 2013). The size in the tail direction is not precisely known.

- Interstellar wind is somewhat disturbed beyond the heliopause forming an interface region, whose exact size is not well-known. An existence of a bow shock as an interface between disturbed and undisturbed interstellar wind was proposed, but recent data disputes that (McComas et al. 2012; Zieger et al. 2013). Beyond this boundary, interstellar wind does not “know” about the presence of an obstacle caused by the solar wind.

The heliospheric structure and conditions can be probed by not only dedicated spacecraft but also by cosmic rays traversing the heliosphere. Cosmic rays near Earth are of two main types: energetic (10^8 – 10^{20} eV/nucleon) galactic cosmic ray (GCR) particles existing all the time but modulated by the solar magnetic activity within the heliosphere; and less energetic (10^6 – 10^{10} eV/nucleon) solar energetic particles (SEP) which occur as sporadic solar proton events (SPEs), when the flux of such particles can be enhanced by many orders of magnitude.

Since the solar magnetic activity depicts a dominant 11-year cycle driven by the solar dynamo (Hathaway 2010), the heliosphere also changes with the 11-year solar cycles. Accordingly, the flux of energetic particles near Earth also varies both within the 11-year solar cycle and on the long-term scale. Here we present a brief review of the solar cycle as reflected in different aspects of the heliospheric and cosmic ray variability near the Earth. Other relevant reviews can be found, e.g., in Balogh et al. (2008).

Although this paper is devoted to the near-Earth observations, it is necessary to mention invaluable contributions of distant space missions to understanding of the heliosphere 3D structure and dynamics. Pioneer 10 (1972–2003), Pioneer 11 (1973–1995) reaching ≈ 80 AU, and Voyager 1 and 2 (both launched in 1977 and now exploring the outer heliosphere and beyond) provide unique data exploring the extreme far regions of the heliosphere. The space probe Ulysses (1990–2009) explored space outside the ecliptic plane, performing three scans over the solar polar regions in 1994–1995, 2000–2001, and 2007–2008, and documenting the 3D structure of the heliosphere. Consideration and discussion of these points can be found in Stone et al. (2005), Heber and Potgieter (2006), Balogh and Erdős (2013), Heber (2013), and Mewaldt (2013).

2 Solar Cycles in the Heliosphere

The very existence and dynamical balance of the heliosphere are ultimately governed by the solar surface activity which is driven by the 11-year cyclic solar dynamo process leading to variations in the solar wind dynamic pressure. As a result, the heliospheric extent (distance to the termination shock in the ecliptic plane) would be maximal on the decline of the cycle when low-latitude high-speed streams are most prominent (e.g., Richardson and Schwadron 2008).

2.1 Solar Wind and Heliospheric Magnetic Field in the Ecliptic Plane

The temporal variability of solar magnetic activity (quantified by the sunspot number—Usoskin 2013; Clette et al. 2014) is shown in Fig. 1 along with the key heliospheric parameters—solar wind speed, proton density, HMF—since 1965.

The heliospheric parameters presented here were measured *in-situ* at the Earth's orbit, i.e. in the ecliptic plane at 1 AU. SSN variability (Fig. 1A) is dominated by the 11-year cycle, varying from nearly no spots at solar minimum to high values of about 200 at solar maximum. To date, current cycle No. 24 which started in December 2008 is only about half as large as the average of cycles 18–23, indicating the end of the Modern Grand Maximum of

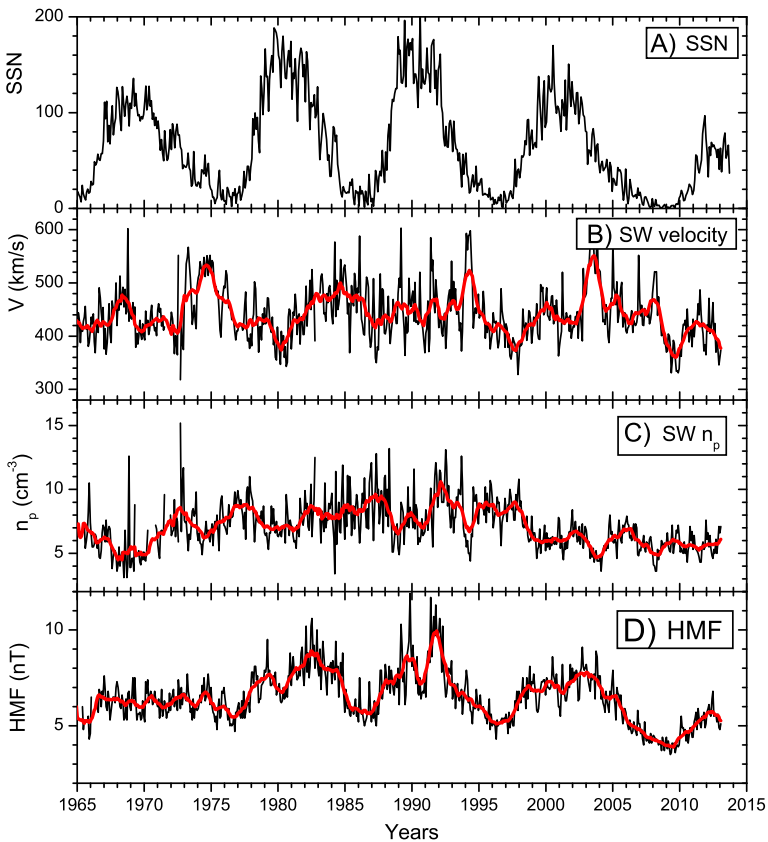
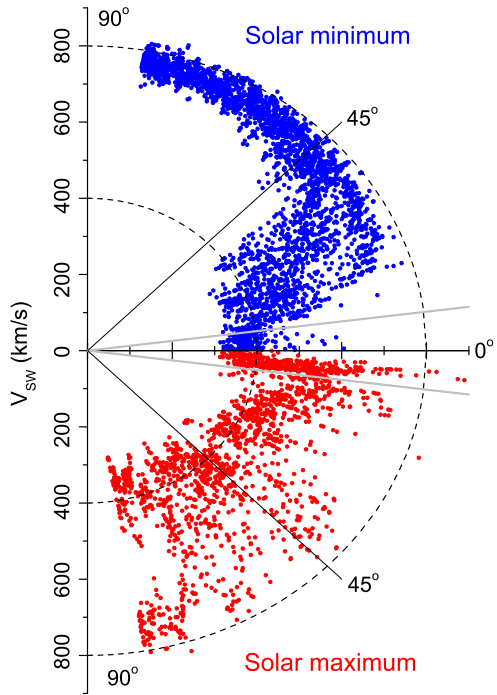


Fig. 1 Variability of the solar and heliospheric parameters for the period 1965–2013. **(A)** Monthly international sunspot numbers (<http://sidc.oma.be/>). **(B)** Solar wind velocity at the Earth's orbit (OMNIweb data <http://omniweb.gsfc.nasa.gov/>). **(C)** Solar wind proton density at the Earth's orbit (OMNIweb data). **(D)** Heliospheric magnetic field HMF at the Earth's orbit (OMNIweb data). *Red curves* depict the running 13-month means

solar activity (Solanki et al. 2004; Usoskin et al. 2007; Clette et al. 2014). On the other hand, heliospheric parameters near Earth show little variability over the solar cycle. Solar wind speed (panel B) does not depict a clear 11-year cyclic variability. Richardson et al. (2002) found that “For minimum periods, the Earth is embedded in high-speed streams $\approx 55\%$ of the time (most prominently on the decline of the cycle) versus $\approx 35\%$ for slow solar wind and 10% for coronal mass ejection (CME)-associated-structures, while at solar maximum, typical percentages are as follows: high-speed streams $\approx 35\%$, slow solar wind $\approx 30\%$, and CME-associated $\approx 35\%$.” Thus the strongest sustained high-speed wind characteristically occurs on the decay of the sunspot curve. Proton density (panel C) also does not show a signature of the 11-year cycle, although a tendency of reduced density during the current weak cycle can be observed. The HMF does show a 11-year cycle of a factor of two as the max-min ratio. It is notable that HMF is weaker during the current cycle reaching the lowest measured value of about 3.5 nT in 2009. The HMF changes its dipole polarity near solar sunspot maximum time every solar cycle leading to the 22-year magnetic cycle called the Hale cycle (Cliver 2014). For more detail see a review by Owens and Forsyth (2013).

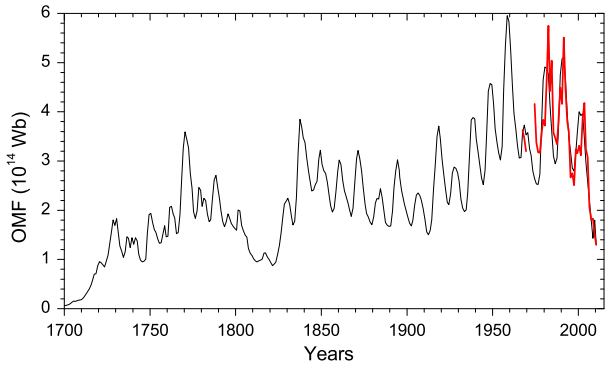
Fig. 2 Heliolatitudinal distribution of the daily solar wind velocities measured by Ulysses spacecraft (data from OMNIweb). The upper (blue dots) and lower (red dots) panels are built for the solar minimum (1994–1997 and 2005–2009) and solar maximum (1991, 2000–2003) conditions, respectively. The plot is given in polar coordinates, where the radial distance represents the solar wind speed in km/s, while the polar angle corresponds to the heliolatitude. The horizontal central line is the heliomagnetic equator, while the grey lines denote the range of the ecliptic zone in the heliocentric coordinates



2.2 3D View

Since the ecliptic plane is close to the solar equator (slightly tilted with about 7° inclination), it is a special region, and the heliospheric values measured in the ecliptic plane may not be fully representative for the full 3D heliosphere. Because of the tilt between the ecliptic plane and the helio-equator, the Earth scans a narrow range of heliolatitudes ($\approx 14^\circ$) around the heliomagnetic equator (bounded by the grey lines in the Fig. 2) within one year. However, this scan is too narrow to give a flavor of the full 3D variability of the solar wind. While HMF in the ecliptic plane is roughly representative for the entire heliosphere (Lockwood 2013), the solar wind velocity varies dramatically at different helio-latitudes. Figure 2 summarizes the observations made onboard the Ulysses spacecraft during its latitudinal scans of the heliosphere (Wenzel et al. 1992). The upper panel (blue dots) shows the solar wind velocity for the solar minimum condition. A clear pattern is observed—slow solar wind dominates at low heliolatitudes, while fast solar wind dominates at high latitudes (McComas et al. 2008). This structure is caused by the presence of large unipolar coronal holes in the Sun's polar regions that emit fast solar wind. The situation is dramatically changed around solar maxima (lower panel of Fig. 2), when a mixture of fast and solar wind streams appear, caused by widespread small coronal holes and CME activity. Therefore, the solar wind as measured in the ecliptic plane is not representative for the full heliosphere. Moreover, the cyclic variability of the solar wind velocity at the ecliptic plane (slow solar wind at solar minima and more frequent fast solar wind streams at late declining phase of the solar cycle) is opposite to the higher latitude pattern.

Fig. 3 Time variability of the open magnetic flux since the Maunder minimum of solar activity, reconstructed (*black line*—Vieira and Solanki 2010) and computed from *in situ* measurements (*red line*—Lockwood et al. 2009)



2.3 Open Solar Magnetic Flux

An important factor for the cosmic rays in the heliosphere is the open magnetic flux (OMF) of the Sun (Cane et al. 1999; Cliver and Ling 2001b; Lockwood 2013), which can be calculated from the parameters measured *in situ* near Earth or from the solar surface magnetic maps, and then recalculated to the OMF at the source surface at 2.5 solar radii around the Sun. OMF shows a great variability both in solar cycle and on the centennial scale (see Fig. 3). It is important to note that the centennial variability is great (Lockwood et al. 1999; Solanki et al. 2000) comparable with or even greater than the 11-year cycle range of variability. It is noteworthy that the recent solar minimum of 2009 yielded low OMF values, comparable to those around 1900 and during the Dalton minimum ca. 1820, indicating the end of the Modern Grand Maximum of solar activity.

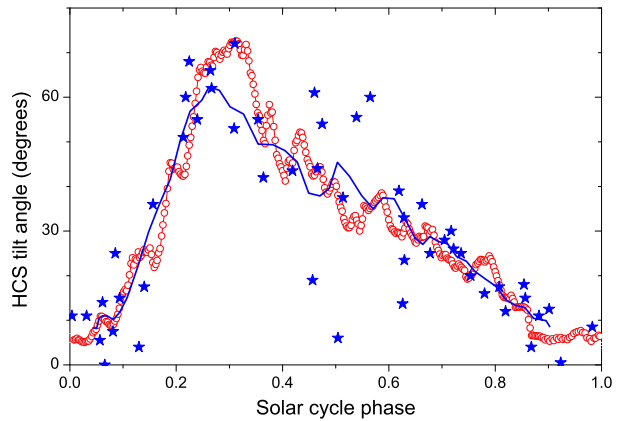
2.4 Heliospheric Current Sheet

A specific feature of the heliospheric structure, which is very important for cosmic ray modulation (Potgieter 2013), is the heliospheric current sheet (HCS) which is a thin shear interface separating the regions of the opposite polarity of HMF emerging from the Sun. It corresponds to the heliomagnetic equator. Since the magnetic dipole axis of the Sun is tilted with respect to rotational axis, this together with the Sun's rotation and radially expanding solar wind, leads to formation of a complicated 3D-structure, resembling a ballerina's skirt (Mursula and Hiltula 2003; Owens and Forsyth 2013). The waviness of HCS, which plays an important role in GCR modulation (Alanko-Huotari et al. 2007b), is defined by the tilt angle, which varies cyclically over the solar cycle so that the HCS is nearly flat around the solar minimum and reaches its maximum values of above 70° around solar maximum times (Fig. 4). Direct computations of the tilt angle started in mid-1970s but indirect estimates (Pishkalo 2006) can be done even before that based on observations of solar eclipses since 1870 (Fig. 4). The results suggest that the cyclic variability of the HCS warp does not depend on the strength of the solar cycle—the tilt angle varies to its full extent for both high (in the second half of 20th century) and low (ca. 1900) solar cycles. It does not depict a centennial variation. Accordingly, we may expect a similar pattern, for example for the Maunder minimum condition.

2.5 Grand Minima of Solar Activity

Of special interest is a question what are the heliospheric conditions during a grand minimum of solar activity, the most famous example being the Maunder minimum in 1645–1700

Fig. 4 Variability of the HCS tilt angle as a function of the 11-year solar cycle phase. The *red dots* represent the HCS tilt angle (radial model) averaged over cycles 21–23 (Wilcox Solar Observatory <http://wso.stanford.edu/Tilts.html>), the *blue stars* depict the tilt angle reconstructed from solar eclipses since 1870 (Pishkalo 2006), and the *blue curve* is a 7-point running mean over the *blue stars* (cf. Alanko-Huotari et al. 2007a)



with almost no sunspots on the solar surface (Eddy 1976). Despite the lack of sunspots a weak cyclic variability was observed during the Maunder Minimum in geomagnetic and cosmic ray indices (Beer et al. 1998; Usoskin et al. 2001; Miyahara et al. 2004; Berggren et al. 2009; Owens et al. 2012) suggesting that the solar magnetic cycle was still operating in the heliosphere. Different estimates of the HMF and solar wind parameters exist, but the current paradigm (Cliver et al. 1998; McCracken 2007a; Steinhilber et al. 2010; Owens and Forsyth 2013; Lockwood and Owens 2014) is that the HMF was weak, about 2 nT, and solar wind in the ecliptic plane remained slow as emanating from hot parts of the corona even in the absence of active sunspot regions. The likelihood that the solar wind was slow during the Maunder Minimum was underscored by the recent solar cycle minimum between cycle 23 and 24, when Earth was embedded in slow solar wind $\approx 70\%$ of the time in 2009 (Cliver and Ling 2011). However, because of the imbalance between the different processes, the phase relation between OMF (and hence cosmic rays) and the solar magnetic cycle was probably inverted with respect to normal solar cycles (Owens et al. 2012). Such grand minima occur every now and then (Usoskin 2013) and correspond to a special mode of the solar dynamo (Usoskin et al. 2014).

3 Solar Cycles in Galactic Cosmic Rays as Observed at Earth

In this section we discuss how the conditions in the heliosphere are reflected by the results of cosmic ray observations. Galactic cosmic rays are highly energetic fully ionized nuclei coming into the heliosphere from outside the solar system with a roughly constant flux. GCRs with kinetic energy in the range from a few hundred MeV up to 100 GeV can be regarded as heliospheric probes. Transport of cosmic rays in the heliosphere is governed by several processes, viz. diffusion due to scattering on the HMF irregularities, convection with the radially expanding solar wind plasma, drift in the large-scale heliospheric magnetic field including that along the HCS, and adiabatic energy losses due to the divergence of solar wind (see Potgieter 2013, for details). All these heliospheric characteristics depend on the phase of the solar magnetic cycle and on the solar activity level. As a result, the GCR flux is modulated by the solar magnetic activity. Therefore, by measuring GCR flux at Earth one can study the 11-year and 22-year cycles in the heliosphere.

Figure 5 presents time profiles of SSN as well as GCR intensity as observed by different instruments sensitive to different energy ranges of primary particles. The GCR records vary

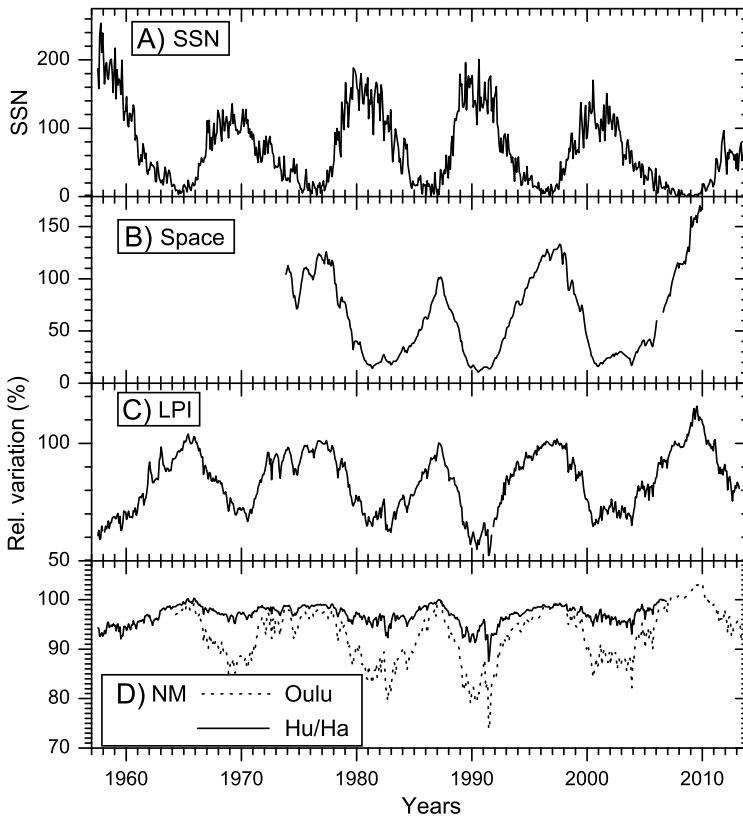


Fig. 5 Time variability of: (A) sunspot numbers (<http://sidc.oma.be/sunspot-data/>); (B) cosmic ray relative intensity measured in space onboard IMP8 and PAMELA spacecraft; (C) cosmic ray relative intensity measured by high latitude balloons (LPI); (D) cosmic ray relative intensity measured by ground-based neutron monitors, polar Oulu and equatorial Huancayo/Haleakala. Relative variations of cosmic rays are normalized to 100 % in March 1987

cyclically in rough anti-phase to SSN with a delay which depends on the direction of the CR drifts in the heliosphere (Usoskin et al. 1998; Cliver and Ling 2001a). The depth of the modulation depends greatly on the CR energy: it varies from a few % for an equatorial NM to ≈ 20 % for a polar NM (see panel D); a factor of two for stratospheric balloon-borne data (panel C); and up to an order of magnitude for space-borne data (panel B). One can also see alternation of sharp and flat peaks in the GCR intensity that is related to the dominant drifts in the heliosphere (Potgieter 2013). An important feature is that the GCR intensity in 2008–2010 was the record high for the entire series reflecting the weak solar activity. The GCR intensities (Fig. 5) follow the (inverted) 11-year solar cycle much better than any individual heliospheric plasma and magnetic field parameter observed in the near Earth space (Fig. 1). On the other hand, GCR flux is well related to the OMF from coronal holes at latitudes $\leq 45^\circ$ (Cliver and Ling 2001b; Alanko-Huotari et al. 2006). This implies that the local *in situ* heliospheric measurements at 1 AU in the ecliptic plane may not necessarily represent the global heliospheric changes, since the GCR modulation is affected by the plasma and magnetic field parameters in the whole heliosphere rather than locally.

3.1 Cosmic Ray Detectors and Their Energy Responses

In order to study the 11-year cycle in CR intensity one needs long-term time series of measurements of the charged particle flux. Since the GCR modulation depends on particle energy, detectors sensitive to different energy ranges of CR are needed. The low energy part of the GCR spectrum, up to tens of GeV, is affected by the heliospheric modulation, but there is an indication that a weak modulation may affect even ≈ 100 GeV particles (Potgieter and Strauss 2013).

In the energy range of 0.5–15 GeV, the geomagnetic field and the Earth's atmosphere serve as an energy separator (see e.g., Grieder 2001). First attempts to initiate a permanent ground-based regular CR observational network, with identical ionization chambers (IC), refer back to 1930s (Forbush 1954). ICs at sea level detect secondary muons generated in the atmosphere by protons with energies >4 GeV impinging at the top of the atmosphere.

However, a real impetus to regular CR monitoring was given by John Simpson with invention of a neutron monitor (Simpson 1958, 2000). A world-wide network of ground-based neutron monitors (NMs) was developed in 1950s and included, in different times, more than a hundred NMs, with more than 40 NMs operating presently (Moraal et al. 2000; Mavromichalaki et al. 2011). The NM data set is available from mid-1950s up to now (see, e.g., Fig. 5d). Because of the geomagnetic shielding, each NM accepts particles above some cut-off energy/rigidity defined by the location of the NM and the geomagnetic field strength. The shielding is absent in polar and maximum in equatorial regions where the cut-off rigidity is about 15 GV. Thus, the global NM network can be considered as a single device allowing to obtain information on the CR particle fluxes, their energy and anisotropy. Reconstructions of the GCR flux based on the NM network data agree well with the direct balloon- and spaceborne measurements, making the NM network a very useful instrument to monitor CR flux (Usoskin et al. 2011).

The problem of converting the data obtained on the ground and in the atmosphere into characteristics of the primary CRs requires knowledge of the response/yield function of different devices and understanding of the atmospheric/magnetospheric transport (e.g., Caballero-Lopez and Moraal 2012). As a measure of the sensitivity of a NM to CR energy, Alanko et al. (2003) introduced a concept of the effective energy for a NM, E_{eff} , such that the count rate of a given NM is proportional to the flux of GCR with energy above E_{eff} , which varies between 6.5 GeV for a polar NM to 30–40 GeV for an equatorial NM.

Another common type of ground-based cosmic-ray detector is a muon telescope measuring the muon component of the cosmic-ray induced atmospheric cascade. They typically have higher effective/median energy (40–60 GeV—see Jämsén et al. 2007) than NMs.

The ground-based monitoring is complemented by CR observations in the Earth's atmosphere. During 1951–1969, Neher (1967, 1971) accomplished a series of regular but infrequent balloon measurements of the cosmic ray induced ionization. In mid-1950s, a Soviet/Russian program (Charakhchyan 1964; Stozhkov et al. 2009) lead by the Lebedev Physical Institute (LPI) of long-term balloon-borne observations of the CR fluxes at several latitudes in the Earth's atmosphere had started and continues till now (see Fig. 5c). Balloons were launched on the daily basis until 1990, and three times a week since then. The LPI balloon measurements get data from the ground level up to the altitude of about 30 km. This data corresponds to $E_{\text{eff}} \approx 1\text{--}2$ GeV (Bazilevskaya et al. 2013).

Numerous balloon-borne detectors have been launched to measure the CR spectrum at shallow atmospheric depth, such as, e.g., BESS instrument (e.g. Shikaze et al. 2007). However, such measurements, while providing direct measurements of the GCR spectrum, are campaign-based and do not provide long-term monitoring.

Cosmic rays with energy below several hundred MeV can be recorded only by spacecraft-borne detectors because such particles are absorbed in the upper atmosphere. Only a few limited data sets of sufficient duration are available, among them the results from the IMP8, and the ACE spacecraft (McDonald 1998; McDonald et al. 2010), and the more recent PAMELA (Adriani et al. 2013) and AMS (Ting 2013) orbital spectrometers. A record is shown in Fig. 5b and corresponds to the flux of protons with energy 120–230 MeV (Bazilevskaya et al. 2013).

3.2 CR Transport in the Heliosphere

Temporal variability of GCR intensity in the energy range affected by solar modulation provides indirect information on the state of the whole heliosphere, not only in the vicinity of Earth. For this purpose, one needs to understand the processes driving the CR transport in the heliosphere. The basics of the CR transport equation were introduced in the 1960s (Parker 1965; Jokipii 1966; Dolginov and Toptygin 1967; Gleeson and Axford 1967; Krymskij 1969) and further developed by a number of groups (e.g., Dorman 2006). Modern CR transport models are sophisticated and precise (for a review see Potgieter 2013, and references therein), allowing to study numerically different effects and processes. In order to study the full process, however, one needs detailed information on the local interstellar spectrum of GCRs, as well as geometrical structure, polarity, strength, and turbulence level of the HMF and the solar-wind speed throughout of the 3D heliosphere. Unfortunately, as discussed above, there are, with rare exceptions, only local near-Earth observations of the HMF parameters. Therefore, the models have to use assumptions, e.g., regarding elements of the diffusion tensor that cannot be measured directly. On the other hand, modulation of GCRs with energy above several hundred MeV can be formally described by the so-called force-field model (e.g., Gleeson and Axford 1968; Caballero-Lopez and Moraal 2004). This model parameterizes the GCR spectrum with a single formal parameter, the modulation potential. The momentary value of the modulation potential can be calculated from the data of the ground-based NM network (Usoskin et al. 2011). On the long-term timescale, the modulation parameter can be reconstructed from data of cosmogenic isotopes ^{14}C and ^{10}Be measured in terrestrial archives (see, e.g., Beer et al. 2012; Usoskin 2013).

It has been demonstrated that this approach, while not pretending to be a physical interpretation, provides a very useful single-parameter parameterization of the GCR energy spectrum near Earth (see formalism in Usoskin et al. 2005), especially for long-term studies. Nonetheless, a more sophisticated approach is needed to give insight into detail of CR interaction with the heliospheric magnetic field.

3.3 CR Diagnostic of the Heliosphere

Modulation of GCR in the heliosphere is largely defined by the turbulent component of HMF responsible for particle diffusion, as the mean free path depends on the power spectrum of the magnetic irregularities in the heliosphere (Jokipii 1966). Recent models (e.g., Ferreira and Potgieter 2004) are good in explaining the temporal variability of the observed GCR fluxes, implying that the basic conception of CR modulation is correct. However, the value of the mean free path remains unknown because of the complicated structure of the turbulent interplanetary magnetic field (Giacalone 2013). The HMF has, in the rough approximation, a form of an Archimedian spiral (Parker 1965) that, leads to gradient and curvature drifts of CR in the interplanetary medium. Account for motion of the magnetic field foot-points on the Sun leads to a more realistic Fisk-type HMF (Fisk 1996) which is particularly important

at high latitudes. Important is also a drift at the HCS which is an extreme case of the gradient drift. The role of the drift effects in CR modulation was pointed out by Jokipii and Levy (1977) and intensively studied since then (e.g., Alanko-Huotari et al. 2007b; Strauss et al. 2012b). When the solar magnetic field is directed outward from the Sun in the north polar region (the so-called $A > 0$ periods), positively-charged particles drift inwards in the heliospheric polar regions and drift outwards along the HCS. This facilitates CR access into the inner heliosphere leading to the long flat shape of CR intensity maxima as, e.g., ca. 1976 and 1996. The drift has the opposite pattern during $A < 0$ periods, forming favorable conditions for the CR access to the inner heliosphere when the HCS is flat. This leads to sharp high peaks of CR intensity in 1965, 1987 and 2009. This drift-dominated modulation is typical (but see the next section) for minima of solar activity cycles when the heliospheric structure is fairly regular. The shape alternation of CR maxima is seen in Fig. 5 as a prominent signature of the drift effect in the CR modulation. However, during periods of high solar activity drifts are less important (Kraivev and Kalinin 2013) since the modulation is mostly driven by diffusion and propagating barriers (Burlaga et al. 1985).

3.4 Unusual Minimum of Solar Activity Between Solar Cycles 23 and 24

As one can see in Fig. 5, the intensity of GCR reached in 2009 its record highest value, over the entire period of direct observations since 1950s (see, e.g., Heber et al. 2009; Ahluwalia et al. 2010; McDonald et al. 2010; Moraal and Stoker 2010; Kraivev et al. 2013). This happened during the minimum of solar activity between solar cycles 23 and 24, which is known to be the weakest heliospheric activity period for the space era (Gibson et al. 2011; McComas et al. 2013). This period is characterized by the record-low HMF intensities, reduced HMF turbulence, change in the inhomogeneity spectrum of the HMF, and reduced solar-wind dynamic pressure. The GCR intensity reached a sharp maximum in 2009 following the flattening of the HCS and then quickly dropped to the normal level after the sudden increase of the HCS tilt angle in early 2010 (McComas et al. 2013). The GCR intensity enhancement was observed in a wide range of particle energies (Fig. 5). It was as great as 60 % at a few hundred MeV energy (panel B) and only a few % in the data of a polar NM (panel D). On the other hand, the CR intensity as recorded at mid- and low-latitudes (geomagnetic cutoff rigidity above 4 GV) did not show any excess in 2009 compared to 1987 (Moraal and Stoker 2010). The unusual rigidity dependence of the GCR increase suggests that significant changes took place in the heliosphere properties during the recent solar cycle minimum (Mewaldt et al. 2010; Bazilevskaya et al. 2012; Kraivev and Kalinin 2013; Potgieter et al. 2014). These facts indicate that mainly lower energy GCRs (≤ 10 GeV) were affected by the favorable heliospheric conditions but not higher energies (see, e.g. Usoskin et al. 2011). Cliver et al. (2013) pointed out that the record increase in cosmic ray intensity in 2009—which was accompanied by a decrease in HMF and an increase in the tilt angle relative to the previous minimum—challenged the dominance of drift effects for modulation at 11-yr minima of the solar cycle. More recently, Potgieter et al. (2014) concluded that “the 2009 modulation minimum could be described as more ‘diffusion dominated’ than previous solar minima” and that “diffusion contributed ≈ 50 % of the total cosmic proton intensities observed at Earth while particle drifts contributed the other 50 %”. This implies that the scaling of the HMF turbulence changed during the recent solar cycle minimum compared to the previous minimum period, although a more detailed analysis and modelling is required to fully understand this process (Strauss et al. 2012a).

4 Cycles in Solar Energetic Particles

4.1 Solar Proton Events

Unlike many solar and geophysical measurements such as SSN or geomagnetic indices, the history of identification of solar proton events (SPEs) is not as long. The first SPEs were directly recorded by ICs in Cheltenham (USA), Godhavn (Greenland), and Christchurch (New Zealand) in 1942 as clear increases on 28-Feb and 7-Mar (Lange and Forbush 1942). However, these increases were not ascribed to particles from the Sun until the third increase was observed at these same locations on 25-Jul-1946 (Forbush 1946). A fourth increase (19-Nov-1949) was also recorded by other detectors, e.g., by an IC in Climax, USA (Forbush et al. 1950), muon detectors at several locations and a prototype NM at Manchester, UK (Adams 1950). While direct measurements of SPEs prior to the 19th solar cycle were limited to the ICs and early NMs, there were indirect measurements from vertical incidence ionospheric soundings made at high latitude locations starting in 1938. In a comparison of polar cap absorption events in 1956–1959 with records of vertical incidence soundings, Švestka (1966) compiled a fairly homogeneous set of data on strong polar cap absorption events for 1938–1959. During the 19th solar cycle, lower energy SPEs could be identified by ionospheric measurements, and instruments on balloons and early rocket and satellite experiments, that were able to detect solar protons at lower energies (MeV range). The solar proton catalog edited by Švestka and Simon (1975) provides a compendium of SPEs of the 19th solar cycle, which is not, however, intended to provide a homogeneous database; nevertheless it is the best data available during that time period. Similar catalogs were compiled also later under the supervision of Yu.I. Logachev¹ spanning the period of for 1970–1996.

The installation of the standardized NMs starting in 1951 considerably enhanced the ability to detect large relativistic SPEs. The event of 23-Feb-1956 was the largest increase recorded by ground-based NMs and muon detectors: the Leeds NM recorded an increase of 4554 % over a 15-minute interval, and the Moscow muon detector recorded an increase of 300 %. Throughout the 19th solar cycle (1954–1965) ground-based NMs and muon detectors were essentially the only instruments that could identify high energy relativistic SPEs. Accordingly, these events were called ground-level enhancements, or ground-level events (GLEs).

Starting with the IMP satellite program in 1964, it became possible to assemble an almost homogeneous database of SPEs recorded at Earth. In 1976, the NOAA/USAF Space Environment Services Center in Boulder, Colorado defined a significant solar proton event (SEP) as any event with a proton flux greater than 10 protons $(\text{cm}^2 \text{sr})^{-1}$ above 10 MeV. Using this criteria, Shea and Smart (1990) compiled a list of SPEs from 1955 until 1986 (i.e. solar cycles 19–21). While an update of that list is beyond the scope of this paper, the events in solar cycles 22 through cycle 24 (first 5 years) have been included in the following statistics and graphs.

4.1.1 Statistics of Solar Proton Events

Using the NOAA criteria of identifying a SPE (see above) we have identified all events that meet this criteria in solar cycles 19 through year 5 in solar cycle 24. Since the list of SPEs maintained by NOAA does not identify independent injections of solar protons within

¹<http://www.wdcb.ru/stp/data/PRCATFINAL/>.

Table 1 Summary of Solar Proton Events for Solar Cycles 19 through the first five months of Solar Cycle 24, including: start months and duration (in months) of solar cycles, the total number of discrete events, N_{SPE} , total number of GLEs N_{GLE} , percentage of GLE P_{GLE} vs. the SPEs, and the omnidirectional fluence (in 10^{10} cm^{-2}) of $>10 \text{ MeV}$ protons, F_{10}

| Cycle | Start | Duration | N_{SPE} | N_{GLE} | P_{GLE} | F_{10} |
|-------|----------|----------|------------------|------------------|------------------|----------|
| 19 | May 1954 | 126 | 65 | 10 | 15.4 | 7.2 |
| 20 | Nov 1964 | 140 | 72 | 13 | 18.0 | 2.2 |
| 21 | Jul 1976 | 123 | 81 | 12 | 14.8 | 1.8 |
| 22 | Oct 1986 | 120 | 84 | 15 | 17.8 | 5.8 |
| 23 | Oct 1996 | 146 | 103 | 16 | 15.5 | 7.5 |
| 24 | Dec 2008 | 60 | 29 | 1 | 3.4 | 1.2 |

a major episode of activity unless the $>10 \text{ MeV}$ flux falls below the event threshold, we have examined each of the events for independent and additional sources of solar protons. Increases associated with the arrival of interplanetary shocks at Earth were not assumed to be separate events but considered part of the previous identified event. Occasionally a proton-producing region of activity on the far Eastern limb of the Sun can be associated with a small proton enhancement that does not reach the NOAA proton event criteria. When the interplanetary shock from the coronal mass ejection (CME) of such an event arrives at Earth, the additional protons accelerated by the shock may add to the already enhanced flux such that the SPE criteria will be met. While we considered this as a shock associated increase, it will be listed as a proton event on the NOAA listing. An example of this type of event occurred on 23-Jun-2013.

The events we have identified as separate and unique solar proton events were tallied in 12-month arrays starting with the first month of each solar cycle. The start of each solar cycle was taken as the month after the minimum smoothed sunspot number (see Table 1).

The total omnidirectional fluence (time-integrated flux) of $>10 \text{ MeV}$ protons near Earth, denoted as F_{10} , is often considered as a characteristic integral parameter of SPEs. The values of F_{10} for the past 6 solar cycles (cycle 24 incomplete yet) are given in Table 1. These values differ by factors of 4 from cycle to cycle, which can be attributed to the location of the parent solar activity associated with the various increases over a solar cycle (Shea and Smart 2012). For example one strong event, e.g., in August 1972 can completely dominate the total fluence for the entire solar cycle (Shea and Smart 1990).

Figure 6 illustrates the distribution of SPEs throughout solar cycles 19–23 and the first five years of cycle 24. The distribution of events identified by Švestka (1966) for cycles 17–18 are shown in Fig. 7 using the same convention. While caution should be used in utilizing these data for comparison with the modern SPE identification, the distributions shown in Fig. 7 are similar to those shown in Fig. 6. Figure 8 presents the average number of SPEs over solar cycles 19–23 together with the average sunspot number summed over the same time period. While no coherent pattern of the SPE occurrence is seen in Fig. 6 for individual cycles, the overall pattern of the SPE number appears to be consistent with the average sunspot number when summed over five solar cycles. The distribution of GLEs over solar cycles 19–24 is shown in Fig. 9. In comparing it with Fig. 8, it appears that the occurrence of GLEs is more widely distributed over the solar cycle than the $>10 \text{ MeV}$ proton events. This may either reflect a physical difference or low statistics of GLEs in this time period (67 GLEs vs. 405 SPEs). When the four GLEs of solar cycles 17 and 18, observed by muon detectors, are included, this distribution becomes even wider.

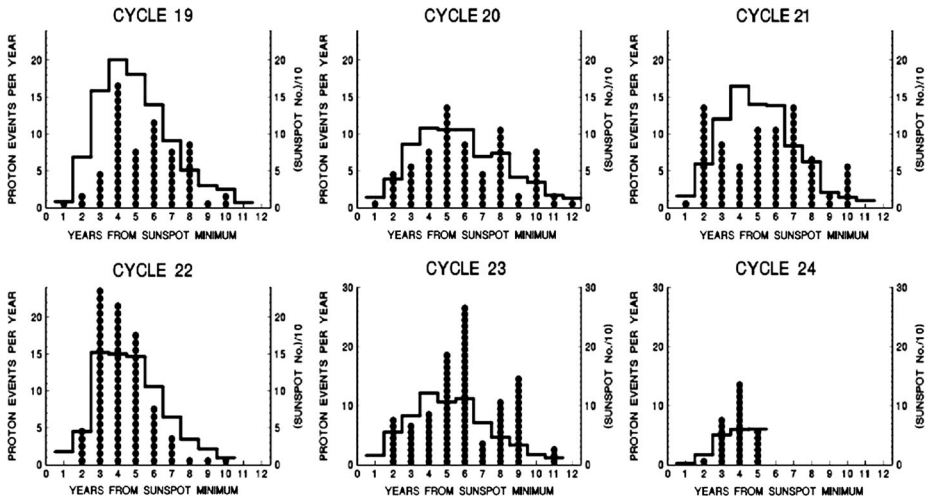


Fig. 6 Distribution of SPEs > 10 MeV over each solar cycle 19–24 (see Table 1 for dates). These are shown in 12-month increments starting with the year after the sunspot minimum for each cycle. Only the first five years of cycle 24 (i.e. through November 2013) are shown. The histograms are the yearly sunspot number (divided by 10) summed for each of the same time periods

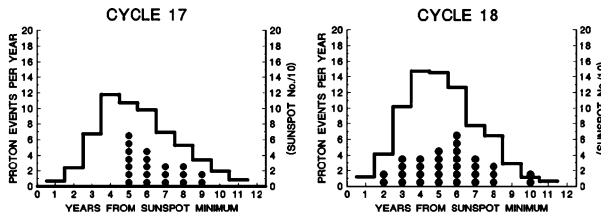


Fig. 7 The distribution of SPEs as identified by Švestka (1966) for solar cycles 17 and 18. The number of events have been binned in 12-month intervals from the start of cycle 17 (October 1933) and the start of cycle 18 (March 1944). The histograms are the yearly sunspot number (divided by 10) summed for each of the same time periods

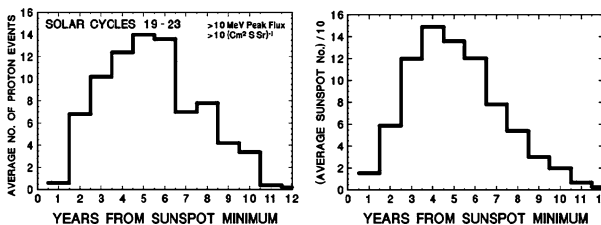
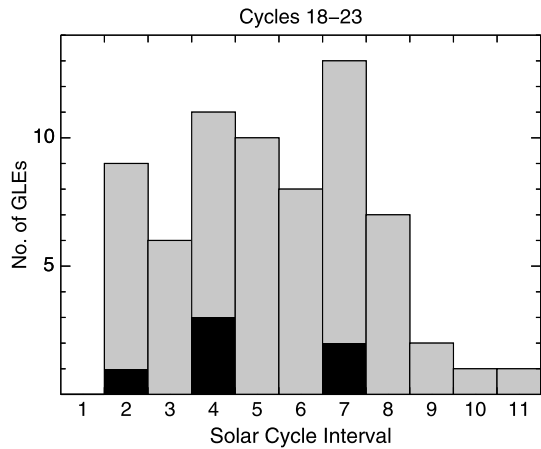


Fig. 8 Left side: Average number of SPEs each year over five solar cycles (1954–2008). Right side: Average sunspot number (divided by 10) over five solar cycles (1954–2008). The yearly values have been calculated for each 12-month period starting with the first month after the minimum value in the smoothed sunspot number

Fig. 9 Occurrence frequency of GLEs over a representative “11-year” solar cycle. Each complete cycle since 1942 has been divided into 11 equal intervals and the number of GLEs has been distributed over the 11 intervals and summed accordingly. The black shading indicates the six GLEs with $F_{200} \geq 3.0 \times 10^7$ proton/cm² from 1956-present (see Sect. 4.3)



4.1.2 Ground Level Enhancements

GLEs are relatively rare events with an almost homogeneous database since 1956, and as such, have been widely studied. Until 2014, there have been 71 GLEs since the first events identified in 1942 with a mean rate of about one event per year (e.g., Cliver et al. 1982; Cliver 2006; Gopalswamy et al. 2012, 2013) but unevenly distributed over the solar cycles (Fig. 10). Ten GLEs were identified in the 19th solar cycle, but a few small events may have been missed because of the anisotropy (not known at that time), the sparsity of detectors particularly in the polar regions, and a low flux of protons >450 MeV to register as an increase on a NM. In the mid 1970s, the cosmic ray community adopted a criterion for an event to be identified as a GLE,² that is two independent NMs have recorded a statistically significant increase. We note that an enhancement of 06-Jan-2014 observed at the South Pole NM (Thakur et al. 2014) was a not a GLE according to the formal criterion. As shown in Fig. 10, these events can occur at any time of the solar cycle but tend to be on the rising and decreasing parts of the cycle. With the exception of solar cycle 22, there is a distinct gap near sunspot maximum indicative of the Gnevyshev Gap (Gnevyshev 1967, 1977).

One important aspect of GLEs is the degree of anisotropy that may be present, particularly for events resulting from solar activity on the western solar hemisphere (see Sect. 3.2 of Shea and Smart 2012). In addition to the normal anisotropy typically present during the first 20–30 minutes of many GLEs, McCracken et al. (2012) have identified high-energy impulsive GLEs that constitute the first phase of some very large GLEs. These authors offered several constraints that must be met by any putative acceleration mechanism for these unusual events. A comprehensive study of GLEs needs to address the degree of anisotropy as well as other defining factors such as the type of detector recording the event, and the geomagnetic cutoff rigidity and altitude of the detector (e.g., Mishev et al. 2014).

While the emphasis on the detection of GLEs since 1955 has been on NM measurements, the importance of the IC and muon measurements should not be ignored even though the particle energies in most GLEs do not have sufficient flux above the 4 GeV threshold for detection by muon detectors. Of the 67 GLEs between 1955 and 2014, only 5 have been recorded by the world wide network of muon detectors as illustrated in Fig. 11. This makes

²The official master list of GLEs is available at <http://gle.oulu.fi>.

Fig. 10 Timing of the 71 GLEs observed from 1942 to the present (*grey bars*) along with sunspot numbers. Solar cycles are separated by *dashed lines*

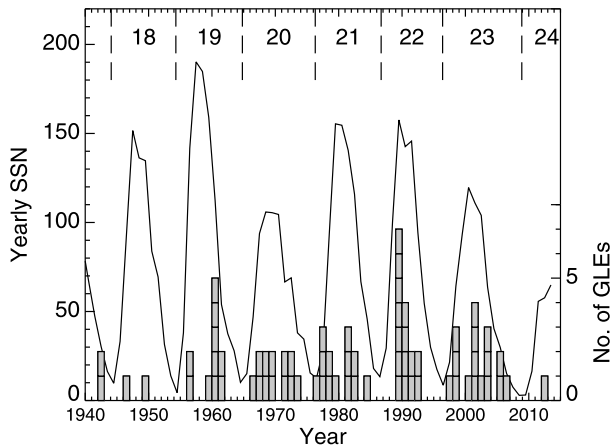
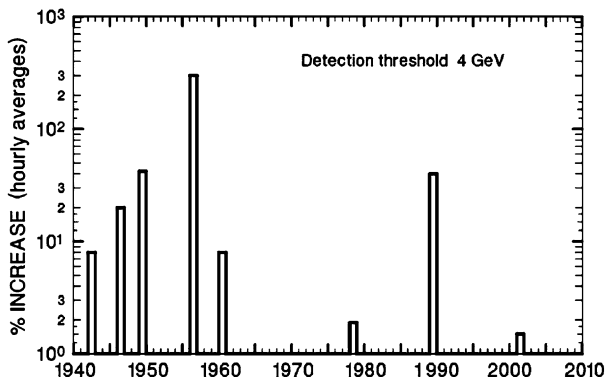


Fig. 11 GLEs recorded by muon detectors (given in percentage increase) at the sea level from 1942 to 2010. The 1940 events are bi-hourly data. The 1950 event are hourly data and the events from 1960 to 2010 are 5 minute data

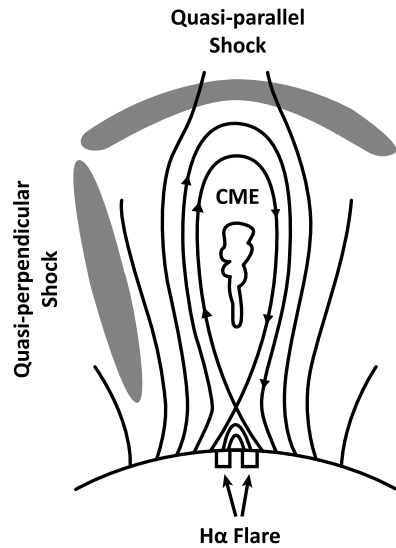


the first four GLEs in solar cycles 17 and 18 very impressive as massive events. The associated solar regions for the events of 28-Feb-1942 and 25-Jul-1946 were located at $\approx 4^\circ \text{E}$ and 15°E respectively (Duggal 1979). The event on 14-Jul-2000 was also associated with central meridian activity (7°W) but the muon detector increase was an order of magnitude lower than for the 1946 event. The remaining events recorded by muon detectors were associated with solar activity on the far western side of the Sun. It should be noted that the increases for the events in the 1940s were from bi-hourly records; hourly data would have more likely been considerably higher.

4.2 Coronal Mass Ejections and SEP Events

It is well-accepted that the free energy for solar activity resides in solar magnetic fields, specifically in the low coronal fields of active regions (e.g., Hudson 2011). Thus, it is not surprising that the source active regions of SPEs powerful enough to be detectable at Earth are generally large. For the 15 GLEs from cycle 23 for which the area of the parent sunspot group could be determined (Cliver 2006; Gopalswamy et al. 2012), the median sunspot area of the GLE-source regions was 750 millionths of a solar hemisphere (msh; range from 360–2580 msh, corrected for foreshortening which reduces the apparent areas of spots away from disk center). As a reference, “naked eye sunspots”, i.e., those that can be seen without

Fig. 12 A schematic view for CME-driven-shock-acceleration of SEPs indicating the locations of quasi-perpendicular and quasi-parallel CME-driven shock acceleration of SEPs (adapted from Cliver 2009b)

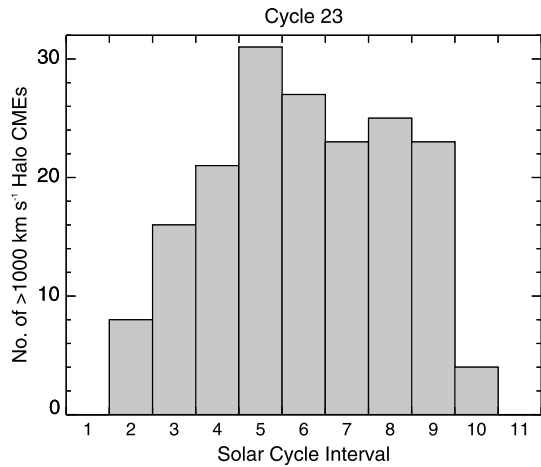


magnification through darkened glass or an atmosphere shielded by light clouds or smoke, have areas of >500 msh and make up only about 5 % of all sunspot groups (Newton 1958).

In the current picture of particle acceleration at the Sun (Reames 1999, 2013; Tylka et al. 2005; Tylka and Lee 2006; Cliver 2009a,b), the high-energy protons that give rise to GLEs are accelerated in solar flares and by CME-driven-shocks, either via diffusive acceleration at a CME bow shock or via shock-drift acceleration at the CME flanks as indicated in the schematic in Fig. 12. To drive the strong shocks associated with GLEs, the CMEs need to be fast and massive. Such CMEs dominate the energy budget of major eruptive flares (Emslie et al. 2012). For example, the CMEs associated with the 16 GLEs of cycle 23 (coronagraph data available for 15) had a median speed of 1810 km/s (range 938–3242 km/s) compared to ≈ 420 km/s for all broad ($>60^\circ$) CMEs in this cycle, while 12 of the 15 CMEs were full halos (Gopalswamy et al. 2009, 2012). The variation in the occurrence of such CMEs (halo CMEs with speeds >1000 km/s) for cycle 23 (1996–2008), for which we have the homogeneous SOHO Large Angle Spectroscopic Coronagraph (Brueckner et al. 1995) data set, is shown in Fig. 13.

The distribution of fast halo CMEs in Fig. 13 looks like the histogram of GLEs over the composite solar cycle for cycles 18–23 in Fig. 9, although the broad maximum of the GLE distribution (spanning intervals 2–8) is shifted one year to the left. The general variation of high-energy SPEs with the solar cycle (Fig. 9) has also been documented for significant SEP events at lower energies (see, e.g., Fig. 8). Comparison of Figs. 13 and 9 (after normalizing for the number of solar cycles) indicates that on average, only 1 of about 15 fast halo CMEs produces a GLE. This significant reduction can have multiple contributing causes. For example, increasing the speed threshold for Fig. 13 to 1500 km/s, closer to the ≈ 1800 km/s median speed for all GLE-associated CMEs during cycle 23, approximately halves the number of fast halo CMEs during this period. Factors unfavorable to SEP acceleration by fast halo CMEs include: low CME brightness (i.e., mass/energy) (Kahler and Vourlidas 2005; Mewaldt et al. 2008), lack of closely-timed preceding CMEs from the same or nearby active regions (Gopalswamy et al. 2002, 2004; Kahler and Vourlidas 2005), low pre-existing seed particle population in the interplanetary medium (Kahler 2001; Tylka et al. 2005; Cliver 2006), and the fact that GLEs are rarely observed from the eastern half of the Sun (only 9

Fig. 13 Histogram of the occurrence of fast (>1000 km/s) halo CMEs over the 11 equal intervals of 13.3 months each, of cycle 23. Corrections to the CME counts were made by prorating for long (>1 month) gaps in coronagraph coverage (vis. 24-Jun-1998–15-Oct-1998 and 20-Dec-1998–5-Feb-1999)



of 71 cases) due to the propagation of SEPs along the Parker spiral (e.g., Shea and Smart 1990).

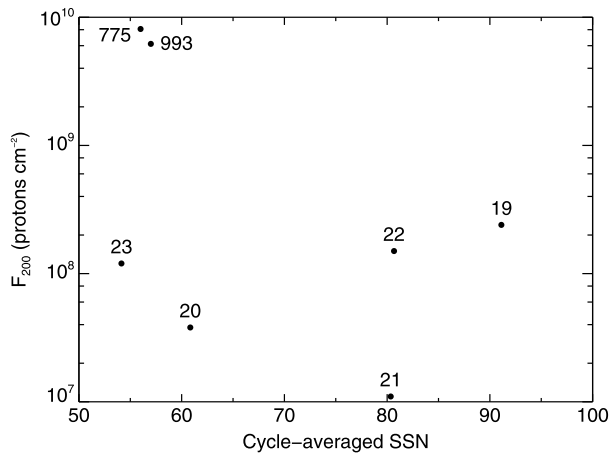
When the parent solar activity (eruptive flare) is near the central meridian of the Sun, a fast CME can propagate outward from the sun accelerating particles as the shock traverses the interplanetary medium between the Sun and Earth. When the parent solar activity is located toward the western limb of the Sun (as viewed from Earth), the time/intensity profiles of these SPEs tend to have rapid rates of rise to maximum intensity followed by a rapid decay. Based upon those observations, Shea and Smart (1994) and Smart et al. (2006) identified a bi-modal distribution of SPEs classified as “interplanetary shock dominated events” and “near-Sun injection events”. For the former, a fast, broad, CME-driven interplanetary shock from activity near the central meridian of the Sun continuously accelerates ions throughout its entire passage from the Sun to Earth. For the lower energy protons (e.g. ≤ 30 MeV) the initial particle flux observed at Earth may be relatively small, but the magnitude continues to increase as the interplanetary shock approaches Earth, often maximizing as the shock passes Earth.

For the “near-Sun injection events” there is identifiable solar activity, preferentially on the western hemisphere of the Sun, with an associated fast CME that typically propagates through the western heliographic longitudes as viewed from Earth. In this type of event, Earth is well connected to the solar active region by the interplanetary magnetic field, and the solar protons can arrive at Earth in a prompt time frame. Solar particle intensity observed at Earth from activity on the western solar hemisphere typically has a faster increase and higher magnitude than similar activity from the central meridian or eastern sector of the Sun (see Fig. 10 in Shea and Smart 1995).

4.3 Variation of High-Energy SEP Events with Long-Term Solar Activity

The era of direct SPE/GLE recording is relatively short and provides little information on the long-term variability. On the other hand, extreme GLE events can be identified as spikes in production of cosmogenic isotope (^{10}Be and ^{14}C) records on the centennial-millennial time scale (e.g., Usoskin and Kovaltsov 2012). For example, the two largest SPE/GLE candidates ever observed (Miyake et al. 2012, 2013; Usoskin et al. 2013; Cliver et al. 2014), were found in 775 AD and 993 AD, as inferred from ^{14}C measured in dendrochronologically-dated tree rings. As shown by Kovaltsov et al. (2014) such spikes are related to the >200 MeV

Fig. 14 Scatter plot of solar cycle totals of F_{200} vs. $\langle \text{SSN} \rangle_{\text{cycle}}$ for cycles 19–23. Points are also plotted for the 775 AD event and 993 AD events with the decadal SSNs encompassing these years taken from Kovaltsov et al. (2014)



fluence in SPEs, F_{200} , as based on SEP spectra from Tylka and Dietrich (2009). Large F_{200} SPEs indicate events with a hard SEP spectrum. The largest F_{200} SPEs since 1950, i.e., those with $F_{200} \geq 3.0 \times 10^7$ proton/ cm^2 , occurred on 23-Feb-1956 (heliolongitude W80), 12-Nov-1960 (W04), 15-Nov-1960 (W35), 29-Sep-1989 (\approx W100), 19-Oct-1989 (E09), and 14-Jul-2000 (W07). McCracken et al. (2012) reported that three of these events, those that originated at solar longitudes \geq W35, exhibited high-energy impulsive peaks (extending to rigidities >5 GV) with short (3–5 minutes) rise times and fall times. They pointed out that, “For a quasi-perpendicular shock such as on the flanks of a CME, it is conceivable that the shock front (sweeping laterally across the face of the Sun) may connect and disconnect with open field lines [nominally near W60] that are connected to Earth, and so lead to both an abrupt switch-on and switch-off of the SEP pulse.” The three large F_{200} events without a reported high-energy impulsive peak all originated near central meridian. For such events the CME-flank-driven shock may not reach the \approx W60 zone of good connection (or may be significantly weaker when it does) and the SEP event can be dominated by the outward expanding quasi-parallel bow shock of the CME. In this case the shock front can remain connected for a longer time to the Parker spiral to Earth, contributing to the extended intensity vs. time profiles observed for SEP events arising from near central meridian (Cane et al. 1988). The black-filled rectangles in the histogram of Fig. 9 show the distribution of the six large F_{200} events over the solar cycle.

Active regions with sunspot areas >1000 msh can occur in even relatively weak solar cycles. For example, in current low-activity cycle 24, the largest active region yet observed had an area of 1580 msh (on 4-Feb-2014). Moreover, at any given proton energy, the fluence from a single large SPE, or a cluster of closely-timed events from the same active region, can dominate the total fluence for a 11-yr cycle. Thus we should not expect SEP fluence over a cycle to be closely tied to the strength of the solar cycle. This can be seen for solar cycles 19–23 in Fig. 14 where F_{200} totals for all GLEs during a given cycle (Kovaltsov et al. 2014) are plotted against the average daily sunspot number for that cycle, $\langle \text{SSN} \rangle_{\text{cycle}}$. No clear dependence of F_{200} on $\langle \text{SSN} \rangle_{\text{cycle}}$ is apparent over the 50–90 range of $\langle \text{SSN} \rangle_{\text{cycle}}$ values for these cycles. In the case of the 775 AD event, the F_{200} fluence for a single event, or cluster of events, exceeded the fluence from the largest solar cycle (No. 19) during the \approx 1945–1995 modern grand maximum (Usoskin et al. 2007; Usoskin 2013) by about a factor of thirty.

Work by McCracken et al. (2004) and McCracken (2007b) implies that if Fig. 14 included smaller cycles with $\langle \text{SSN} \rangle_{\text{cycle}}$ values in the range from 0–50, e.g., for the current

cycle 24 (Richardson 2013), we might see an anticorrelation between F_{200} and $\langle \text{SSN} \rangle_{\text{cycle}}$. Those authors reasoned that less intense cycles would produce a weaker ambient HMF and suggested that CMEs injected into these weaker fields would produce shocks with higher Mach numbers, resulting in more frequent and/or energetic SEP events. At the same time weaker cycles should produce fewer energetic CMEs, partly off-setting the advantage of lower ambient HMF. Thus we see a virtual absence of GLEs during the characteristic intervals of low HMF near sunspot minima because of the relative lack of fast halo CMEs at these times (see years 1 and 11 in Figs. 9 and 13). McCracken and colleagues based their suggestion in part on pre-space-age (e.g., cycles 12–14, 1878–1913) peaks in nitrate concentration in ice cores which they attributed to strong SEP events (McCracken et al. 2001, 2004) and also on four intense GLEs from 1942–1956 during a period of low HMF strength inferred from balloon-borne and ground-based ionization measurements of cosmic rays (McCracken 2007a,b). The ice core evidence, however, has been disputed by Wolff et al. (2012). In addition, the low inferred HMF values circa 1950 inferred from ionization chambers are not substantiated by more recent reconstructions of HMF based on geomagnetic observations (Svalgaard and Cliver 2010; Lockwood and Owens 2011; Kahler 2008) as well as on cosmogenic nuclides (Steinhilber et al. 2010).

Recently, the current weak solar cycle has provided a more direct test of the conjecture of McCracken and colleagues—with mixed results. Gopalswamy et al. (2014) noted the relative absence of GLEs during the rise phase of cycle 24 (see Table 1). They attribute this deficit to reduced total (magnetic plus plasma) pressure in the heliosphere that leads, in turn, to: increased CME lateral expansion, dilution of CME magnetic fields, and less-efficient shock acceleration of SEPs. However, Gopalswamy et al. (2014) also note that while the number of GLEs thus far in cycle 24 is significantly reduced, the overall number (28) of significant > 10 MeV proton events is comparable to that (34) for the corresponding phase of the stronger cycle 23. Following McCracken and colleagues, they suggested that the similarity in the counts of the lower energy SEP events for the two cycles may result from the relative ease of shock formation due to the lower ambient solar wind Alfvén speed in cycle 24, off-setting the size advantage of cycle 23.

The current low cycle is providing valuable data and insight on SEP acceleration during conditions of low solar activity. While significantly more active than the quietest ≈ 50 years of the Maunder Minimum (e.g., Eddy 1976; Usoskin 2013), cycle 24 is giving us our best glimpse to date of SEP activity during periods of low solar activity.

5 Summary

In this concise review we discuss the solar cycle and its manifestations in the heliosphere and cosmic rays.

Most heliospheric parameters are measured *in situ* near Earth, and thus do not straightforwardly represent the entire heliosphere. While some parameters (e.g., HMF) are roughly representative, others (solar wind velocity or plasma density) are not representative for the whole heliosphere. Global heliospheric indices, such as the open magnetic flux are useful in this respect. Galactic cosmic rays can serve as probes of the 3D heliosphere, reflecting its variability on the time scale of 11-year cycle and beyond. The quasi 22-year variability in GCR observed as alternation of top- and flat-peaked cycles is caused by the drift effect of GCR transport in the heliosphere. Special attention is paid upon the recent minimum of solar activity with very quiet heliospheric conditions (low values of HMF and the interplanetary turbulence) which led, together with the flat HCS, to the record high level of GCRs near Earth in 2009.

We also discuss the statistics of the occurrence of SPEs and GLEs that serve as a probe for the inner heliosphere and solar coronal activity. The occurrence of major events depicts an overall tendency to follow the solar cycle but individual events may appear at different phases of the solar cycle, since it is defined not only by the solar energy releases but also by the location of these releases relative to the nominal $\approx W50^\circ$ footpoint of the magnetic fieldline that connects to Earth. We also discuss that the occurrence of major SPEs is not directly related to the overall level of solar activity, and strong events may occur even during moderate solar cycles.

In summary, the solar cycle in the heliosphere and cosmic rays depicts a complex pattern which includes different processes and cannot be described by a simple correlation with sunspot number.

Acknowledgements This work is a result of the ISSI workshop “The Solar Activity Cycle: Physical Causes And Consequences”. G.B. acknowledges support of the RFBR grants 14-02-00905a, 14-02-10006k, 13-02-00585, 13-02-00931, 12-02-00215a and of the “Fundamental Properties of Matter and Astrophysics” Program of the Presidium of the RAS. E.W.C. acknowledges support from AFOSR Task 2301RDZ4. A.G.L. acknowledges support from AFRL contract FA8718-05-C-0036. G.K. was partly supported by the Academy of Finland. I.U.’s contribution is in the framework of the ReSolVE Centre of Excellence (Academy of Finland, project no. 272157). Dr. Clifford Lopate is acknowledged for Huancayo/Haleakala NM data. Oulu NM data is available at <http://cosmicrays oulu.fi>.

References

- N. Adams, A temporary increase in the neutron component of cosmic rays. *Philos. Mag.* **41**, 503–505 (1950)
- O. Adriani, G.C. Barbarino, G.A. Bazilevskaya, R. Bellotti, M. Boezio, E.A. Bogomolov, M. Bongi, V. Bonvicini, S. Borisov, S. Bottai, A. Bruno, F. Cafagna, D. Campana, R. Carbone, P. Carlson, M. Casolino, G. Castellini, M.P. De Pascale, C. De Santis, N. De Simone, V. Di Felice, V. Formato, A.M. Galper, L. Grishantseva, A.V. Karelin, S.V. Koldashov, S. Koldobskiy, S.Y. Krutkov, A.N. Kvashnin, A. Leonov, V. Malakhov, L. Marcelli, A.G. Mayorov, W. Menn, V.V. Mikhailov, E. Mocchiutti, A. Monaco, N. Mori, N. Nikonov, G. Osteria, F. Palma, P. Papini, M. Pearce, P. Picozza, C. Pizzolotto, M. Ricci, S.B. Ricciarini, L. Rossetto, R. Sarkar, M. Simon, R. Sparvoli, P. Spillantini, Y.I. Stozhkov, A. Vacchi, E. Vannuccini, G. Vasilyev, S.A. Voronov, Y.T. Yurkin, J. Wu, G. Zampa, N. Zampa, V.G. Zverev, M.S. Potgieter, E.E. Vos, Time dependence of the proton flux measured by PAMELA during the 2006 July–2009 December solar minimum. *Astrophys. J.* **765**, 91 (2013). doi:[10.1088/0004-637X/765/2/91](https://doi.org/10.1088/0004-637X/765/2/91)
- H.S. Ahluwalia, M.M. Fikani, R.C. Ygbuhay, Rigidity dependence of 11 year cosmic ray modulation: implication for theories. *J. Geophys. Res.* **115**, 07101 (2010). doi:[10.1029/2009JA014798](https://doi.org/10.1029/2009JA014798)
- K. Alanko, I.G. Usoskin, K. Mursula, G.A. Kovaltsov, Heliospheric modulation strength: effective neutron monitor energy. *Adv. Space Res.* **32**, 615–620 (2003)
- K. Alanko-Huotari, K. Mursula, I.G. Usoskin, G.A. Kovaltsov, Global heliospheric parameters and cosmic-ray modulation: an empirical relation for the last decades. *Sol. Phys.* **238**, 391–404 (2006). doi:[10.1007/s11207-006-0233-z](https://doi.org/10.1007/s11207-006-0233-z)
- K. Alanko-Huotari, I.G. Usoskin, K. Mursula, G.A. Kovaltsov, Cyclic variations of the heliospheric tilt angle and cosmic ray modulation. *Adv. Space Res.* **40**, 1064–1069 (2007a). doi:[10.1016/j.asr.2007.02.007](https://doi.org/10.1016/j.asr.2007.02.007)
- K. Alanko-Huotari, I.G. Usoskin, K. Mursula, G.A. Kovaltsov, Stochastic simulation of cosmic ray modulation including a wavy heliospheric current sheet. *J. Geophys. Res.* **112**, 08101 (2007b). doi:[10.1029/2007JA012280](https://doi.org/10.1029/2007JA012280)
- A. Balogh, G. Erdős, The heliospheric magnetic field. *Space Sci. Rev.* **176**, 177–215 (2013). doi:[10.1007/s11214-011-9835-3](https://doi.org/10.1007/s11214-011-9835-3)
- A. Balogh, L.J. Lanzerotti, S.T. Suess, *The Heliosphere Through the Solar Activity Cycle* (Springer, Chichester, 2008). doi:[10.1007/978-3-540-74302-6](https://doi.org/10.1007/978-3-540-74302-6)
- G.A. Bazilevskaya, M.B. Krainev, V.S. Makmutov, Y.I. Stozhkov, A.K. Svirzhevskaya, N.S. Svirzhevsky, Change in the rigidity dependence of the galactic cosmic ray modulation in 2008–2009. *Adv. Space Res.* **49**, 784–790 (2012). doi:[10.1016/j.asr.2011.12.002](https://doi.org/10.1016/j.asr.2011.12.002)
- G.A. Bazilevskaya, M.B. Krainev, A.K. Svirzhevskaya, N.S. Svirzhevsky, Galactic cosmic rays and parameters of the interplanetary medium near solar activity minima. *Cosm. Res.* **51**, 29–36 (2013). doi:[10.1134/S0010952513010012](https://doi.org/10.1134/S0010952513010012)

- J. Beer, S. Tobias, N. Weiss, An active Sun throughout the Maunder minimum. *Sol. Phys.* **181**, 237–249 (1998)
- J. Beer, K. McCracken, R. von Steiger, *Cosmogenic Radionuclides: Theory and Applications in the Terrestrial and Space Environments* (Springer, Berlin, 2012)
- A.-M. Berggren, J. Beer, G. Possnert, A. Aldahan, P. Kubik, M. Christl, S.J. Johnsen, J. Abreu, B.M. Vinther, A 600-year annual ^{10}Be record from the NGRIP ice core, Greenland. *Geophys. Res. Lett.* **36**, 11801 (2009)
- G.E. Brueckner, R.A. Howard, M.J. Koomen, C.M. Korendyke, D.J. Michels, J.D. Moses, D.G. Socker, K.P. Dere, P.L. Lamy, A. Llebaria, M.V. Bout, R. Schwenn, G.M. Simnett, D.K. Bedford, C.J. Eyles, The Large Angle Spectroscopic Coronagraph (LASCO). *Sol. Phys.* **162**, 357–402 (1995). doi:[10.1007/BF00733434](https://doi.org/10.1007/BF00733434)
- L.F. Burlaga, M.L. Goldstein, F.B. McDonald, A.J. Lazarus, Cosmic ray modulation and turbulent interaction regions near 11 AU. *J. Geophys. Res.* **90**, 12027–12039 (1985). doi:[10.1029/JA090iA12p12027](https://doi.org/10.1029/JA090iA12p12027)
- R.A. Caballero-Lopez, H. Moraal, Limitations of the force field equation to describe cosmic ray modulation. *J. Geophys. Res.* **109**, 01101 (2004). doi:[10.1029/2003JA010098](https://doi.org/10.1029/2003JA010098)
- R.A. Caballero-Lopez, H. Moraal, Cosmic-ray yield and response functions in the atmosphere. *J. Geophys. Res.* **117** (2012). doi:[10.1029/2012JA017794](https://doi.org/10.1029/2012JA017794)
- H.V. Cane, D.V. Reames, T.T. von Roseninge, The role of interplanetary shocks in the longitude distribution of solar energetic particles. *J. Geophys. Res.* **93**, 9555–9567 (1988). doi:[10.1029/JA093iA09p09555](https://doi.org/10.1029/JA093iA09p09555)
- H.V. Cane, G. Wibberenz, I.G. Richardson, T.T. von Roseninge, Cosmic ray modulation and the solar magnetic field. *Geophys. Res. Lett.* **26**, 565–568 (1999). doi:[10.1029/1999GL900032](https://doi.org/10.1029/1999GL900032)
- A.N. Charakhchyan, Reviews of topical problems: investigation of stratosphere cosmic ray intensity fluctuations induced by processes on the Sun. *Sov. Phys. Usp.* **7**, 358–374 (1964)
- F. Clette, L. Svalgaard, J.M. Vaquero, E.W. Cliver, Revisiting the sunspot number: a 400-year perspective on the solar cycle. *Space Sci. Rev.* (2014, this issue). doi:[10.1007/s11214-014-0074-2](https://doi.org/10.1007/s11214-014-0074-2)
- E.W. Cliver, The unusual relativistic solar proton events of 1979 August 21 and 1981 May 10. *Astrophys. J.* **639**, 1206–1217 (2006). doi:[10.1086/499765](https://doi.org/10.1086/499765)
- E.W. Cliver, A revised classification scheme for solar energetic particle events. *Cent. Eur. Astrophys. Bull.* **33**, 253–270 (2009a)
- E.W. Cliver, History of research on solar energetic particle (SEP) events: the evolving paradigm, in *IAU Symposium*, ed. by N. Gopalswamy, D.F. Webb, vol. 257 (2009b), pp. 401–412. doi:[10.1017/S1743921309029639](https://doi.org/10.1017/S1743921309029639)
- E.W. Cliver, The extended cycle of solar activity and the Sun's 22-yr magnetic cycle. *Space Sci. Rev.* (2014, this issue). doi:[10.1007/s11214-014-0093-2](https://doi.org/10.1007/s11214-014-0093-2)
- E.W. Cliver, A.G. Ling, 22 year patterns in the relationship of sunspot number and tilt angle to cosmic-ray intensity. *Astrophys. J. Lett.* **551**, 189–192 (2001a). doi:[10.1086/320022](https://doi.org/10.1086/320022)
- E.W. Cliver, A.G. Ling, Coronal mass ejections, open magnetic flux, and cosmic-ray modulation. *Astrophys. J.* **556**, 432–437 (2001b). doi:[10.1086/321570](https://doi.org/10.1086/321570)
- E.W. Cliver, A.G. Ling, The floor in the solar wind magnetic field revisited. *Sol. Phys.* **274**, 285–301 (2011). doi:[10.1007/s11207-010-9657-6](https://doi.org/10.1007/s11207-010-9657-6)
- E.W. Cliver, S.W. Kahler, M.A. Shea, D.F. Smart, Injection onsets of 2 GeV protons, 1 MeV electrons, and 100 keV electrons in solar cosmic ray flares. *Astrophys. J.* **260**, 362–370 (1982). doi:[10.1086/160261](https://doi.org/10.1086/160261)
- E.W. Cliver, V. Boriakoff, K.H. Bounar, Geomagnetic activity and the solar wind during the Maunder minimum. *Geophys. Res. Lett.* **25**, 897–900 (1998). doi:[10.1029/98GL00500](https://doi.org/10.1029/98GL00500)
- E.W. Cliver, I.G. Richardson, A.G. Ling, Solar drivers of 11-yr and long-term cosmic ray modulation. *Space Sci. Rev.* **176**, 3–19 (2013). doi:[10.1007/s11214-011-9746-3](https://doi.org/10.1007/s11214-011-9746-3)
- E.W. Cliver, A.J. Tylka, W.F. Dietrich, A.G. Ling, On a solar origin for the cosmogenic nuclide event of 775 AD. *Astrophys. J.* **781**, 32 (2014). doi:[10.1088/0004-637X/781/1/32](https://doi.org/10.1088/0004-637X/781/1/32)
- A.Z. Dolginov, I. Toptygin, Multiple scattering of particles in a magnetic field with random inhomogeneities. *Sov. Phys. JETP* **24**, 1195 (1967)
- L.I. Dorman, *Cosmic Ray Interactions, Propagation, and Acceleration in Space Plasmas* (Kluwer Academic, Dordrecht, 2006)
- S.P. Duggal, Relativistic solar cosmic rays. *Rev. Geophys. Space Phys.* **17**, 1021–1058 (1979). doi:[10.1029/RG017i005p01021](https://doi.org/10.1029/RG017i005p01021)
- J.A. Eddy, The Maunder minimum. *Science* **192**, 1189–1202 (1976)
- A.G. Emslie, B.R. Dennis, A.Y. Shih, P.C. Chamberlin, R.A. Mewaldt, C.S. Moore, G.H. Share, A. Vourlidas, B.T. Welsch, Global energetics of thirty-eight large solar eruptive events. *Astrophys. J.* **759**, 71 (2012). doi:[10.1088/0004-637X/759/1/71](https://doi.org/10.1088/0004-637X/759/1/71)
- S.E.S. Ferreira, M.S. Potgieter, Long-term cosmic-ray modulation in the heliosphere. *Astrophys. J.* **603**, 744–752 (2004). doi:[10.1086/381649](https://doi.org/10.1086/381649)

- L.A. Fisk, Motion of the footpoints of heliospheric magnetic field lines at the Sun: implications for recurrent energetic particle events at high heliographic latitudes. *J. Geophys. Res.* **101**, 15547–15554 (1996). doi:[10.1029/96JA01005](https://doi.org/10.1029/96JA01005)
- S.E. Forbush, Three unusual cosmic-ray increases possibly due to charged particles from the Sun. *Phys. Rev.* **70**, 771–772 (1946). doi:[10.1103/PhysRev.70.771](https://doi.org/10.1103/PhysRev.70.771)
- S.E. Forbush, World-wide cosmic-ray variations, 1937–1952. *J. Geophys. Res.* **59**, 525–542 (1954)
- S.E. Forbush, T.B. Stinchcomb, M. Schein, The extraordinary increase of cosmic-ray intensity on November 19, 1949. *Phys. Rev.* **79**, 501–504 (1950). doi:[10.1103/PhysRev.79.501](https://doi.org/10.1103/PhysRev.79.501)
- J. Giacalone, Cosmic-ray transport and interaction with shocks. *Space Sci. Rev.* **176**, 73–88 (2013). doi:[10.1007/s11214-011-9763-2](https://doi.org/10.1007/s11214-011-9763-2)
- S.E. Gibson, G. de Toma, B. Emery, P. Riley, L. Zhao, Y. Elsworth, R.J. Leamon, J. Lei, S. McIntosh, R.A. Mewaldt, B.J. Thompson, D. Webb, The whole heliosphere interval in the context of a long and structured solar minimum: an overview from Sun to Earth. *Sol. Phys.* **274**, 5–27 (2011). doi:[10.1007/s11207-011-9921-4](https://doi.org/10.1007/s11207-011-9921-4)
- L.J. Gleeson, W.I. Axford, Cosmic rays in the interplanetary medium. *Astrophys. J. Lett.* **149**, 115 (1967). doi:[10.1086/180070](https://doi.org/10.1086/180070)
- L.J. Gleeson, W.I. Axford, Solar modulation of galactic cosmic rays. *Astrophys. J.* **154**, 1011–1026 (1968)
- M.N. Gnevyshev, On the 11-years cycle of solar activity. *Sol. Phys.* **1**, 107–120 (1967). doi:[10.1007/BF00150306](https://doi.org/10.1007/BF00150306)
- M.N. Gnevyshev, Essential features of the 11-year solar cycle. *Sol. Phys.* **51**, 175–183 (1977). doi:[10.1007/BF00240455](https://doi.org/10.1007/BF00240455)
- N. Gopalswamy, S. Yashiro, G. Michalek, M.L. Kaiser, R.A. Howard, D.V. Reames, R. Leske, T. von Roseninge, Interacting coronal mass ejections and solar energetic particles. *Astrophys. J. Lett.* **572**, 103–107 (2002). doi:[10.1086/341601](https://doi.org/10.1086/341601)
- N. Gopalswamy, S. Yashiro, S. Krucker, G. Stenborg, R.A. Howard, Intensity variation of large solar energetic particle events associated with coronal mass ejections. *J. Geophys. Res.* **109**, 12105 (2004). doi:[10.1029/2004JA010602](https://doi.org/10.1029/2004JA010602)
- N. Gopalswamy, S. Yashiro, G. Michalek, G. Stenborg, A. Vourlidis, S. Freeland, R. Howard, The SOHO/LASCO CME catalog. *Earth Moon Planets* **104**, 295–313 (2009). doi:[10.1007/s11038-008-9282-7](https://doi.org/10.1007/s11038-008-9282-7)
- N. Gopalswamy, H. Xie, S. Yashiro, S. Akiyama, P. Mäkelä, I.G. Usoskin, Properties of ground level enhancement events and the associated solar eruptions during solar cycle 23. *Space Sci. Rev.* **171**, 23–60 (2012). doi:[10.1007/s11214-012-9890-4](https://doi.org/10.1007/s11214-012-9890-4)
- N. Gopalswamy, H. Xie, S. Akiyama, S. Yashiro, I.G. Usoskin, J.M. Davila, The first ground level enhancement event of solar cycle 24: direct observation of shock formation and particle release heights. *Astrophys. J. Lett.* **765**, 30 (2013). doi:[10.1088/2041-8205/765/2/L30](https://doi.org/10.1088/2041-8205/765/2/L30)
- N. Gopalswamy, S. Akiyama, S. Yashiro, G. Michalek, H. Xie, P. Mäkelä, *Geophys. Res. Lett.* (2014, submitted)
- P.K.F. Grieder, *Cosmic Rays at Earth* (Elsevier Science, Amsterdam, 2001)
- D.H. Hathaway, The solar cycle. *Living Rev. Sol. Phys.* **7**(1) (2010). <http://www.livingreviews.org/lrsp-2010-1>
- B. Heber, Cosmic rays through the solar hale cycle. Insights from Ulysses. *Space Sci. Rev.* **176**, 265–278 (2013). doi:[10.1007/s11214-011-9784-x](https://doi.org/10.1007/s11214-011-9784-x)
- B. Heber, M.S. Potgieter, Cosmic rays at high heliolatitudes. *Space Sci. Rev.* **127**, 117–194 (2006). doi:[10.1007/s11214-006-9085-y](https://doi.org/10.1007/s11214-006-9085-y)
- B. Heber, A. Kopp, J. Gieseler, R. Müller-Mellin, H. Fichtner, K. Scherer, M.S. Potgieter, S.E.S. Ferreira, Modulation of galactic cosmic ray protons and electrons during an unusual solar minimum. *Astrophys. J.* **699**, 1956–1963 (2009). doi:[10.1088/0004-637X/699/2/1956](https://doi.org/10.1088/0004-637X/699/2/1956)
- H.S. Hudson, Global properties of solar flares. *Space Sci. Rev.* **158**, 5–41 (2011). doi:[10.1007/s11214-010-9721-4](https://doi.org/10.1007/s11214-010-9721-4)
- T. Jämsén, I.G. Usoskin, T. Rähkä, J. Sarkamo, G.A. Kovaltsov, Case study of Forbush decreases: energy dependence of the recovery. *Adv. Space Res.* **40**, 342–347 (2007). doi:[10.1016/j.asr.2007.02.025](https://doi.org/10.1016/j.asr.2007.02.025)
- J.R. Jokipii, Cosmic-ray propagation. I. Charged particles in a random magnetic field. *Astrophys. J.* **146**, 480 (1966). doi:[10.1086/148912](https://doi.org/10.1086/148912)
- J.R. Jokipii, E.H. Levy, Effects of particle drifts on the solar modulation of galactic cosmic rays. *Astrophys. J. Lett.* **213**, 85–88 (1977). doi:[10.1086/182415](https://doi.org/10.1086/182415)
- S.W. Kahler, The correlation between solar energetic particle peak intensities and speeds of coronal mass ejections: effects of ambient particle intensities and energy spectra. *J. Geophys. Res.* **106**, 20947–20956 (2001). doi:[10.1029/2000JA002231](https://doi.org/10.1029/2000JA002231)
- S.W. Kahler, Prospects for future enhanced solar energetic particle events and the effects of weaker heliospheric magnetic fields. *J. Geophys. Res.* **113**, 11102 (2008). doi:[10.1029/2008JA013168](https://doi.org/10.1029/2008JA013168)

- S.W. Kahler, A. Vourlidas, Fast coronal mass ejection environments and the production of solar energetic particle events. *J. Geophys. Res.* **110**, 12-01 (2005). doi:[10.1029/2005JA011073](https://doi.org/10.1029/2005JA011073)
- G.A. Kovaltsov, I.G. Usoskin, E.W. Cliver, W.F. Dietrich, A.J. Tylka, Relation between >200 MeV solar energetic protons and atmospheric production of cosmogenic radionuclides. *Sol. Phys.* (2014). doi:[10.1007/s11207-014-0093-0](https://doi.org/10.1007/s11207-014-0093-0)
- M.B. Krainev, M.S. Kalinin, On the description of the 11- and 22-year cycles in the GCR intensity. *J. Phys. Conf. Ser.* **409**(1), 012155 (2013). doi:[10.1088/1742-6596/409/1/012155](https://doi.org/10.1088/1742-6596/409/1/012155)
- M.B. Krainev, G.A. Bazilevskaya, S.K. Gerasimova, P.A. Krivoschapkin, G.F. Krymsky, S.A. Starodubtsev, Y.I. Stozhkov, N.S. Svirzhevsky, On the status of the sunspot and magnetic cycles in the galactic cosmic ray intensity. *J. Phys. Conf. Ser.* **409**(1), 012016 (2013). doi:[10.1088/1742-6596/409/1/012016](https://doi.org/10.1088/1742-6596/409/1/012016)
- G.F. Krymskij, *Modulation of Cosmic Rays in Interplanetary Space* (1969)
- I. Lange, S.E. Forbush, Further note on the effect on cosmic-ray intensity of the magnetic storm of March 1, 1942. *Terr. Magn. Atmos. Electr.* **47**, 331 (1942). doi:[10.1029/TE047i004p00331](https://doi.org/10.1029/TE047i004p00331)
- M. Lockwood, Reconstruction and prediction of variations of the open solar magnetic flux and interplanetary conditions. *Living Rev. Sol. Phys.* **10**, 4 (2013). doi:[10.12942/lrsp-2013-4](https://doi.org/10.12942/lrsp-2013-4)
- M. Lockwood, M.J. Owens, Centennial changes in the heliospheric magnetic field and open solar flux: the consensus view from geomagnetic data and cosmogenic isotopes and its implications. *J. Geophys. Res.* **116**, 04109 (2011). doi:[10.1029/2010JA016220](https://doi.org/10.1029/2010JA016220)
- M. Lockwood, M.J. Owens, Implications of the recent low solar minimum for the solar wind during the Maunder minimum. *Astrophys. J. Lett.* **781**, 7 (2014). doi:[10.1088/2041-8205/781/1/L7](https://doi.org/10.1088/2041-8205/781/1/L7)
- M. Lockwood, R. Stamper, M.N. Wild, A doubling of the Sun's coronal magnetic field during the past 100 years. *Nature* **399**, 437–439 (1999). doi:[10.1038/20867](https://doi.org/10.1038/20867)
- M. Lockwood, A.P. Rouillard, I.D. Finch, The rise and fall of open solar flux during the current Grand Solar Maximum. *Astrophys. J.* **700**, 937–944 (2009). doi:[10.1088/0004-637X/700/2/937](https://doi.org/10.1088/0004-637X/700/2/937)
- H. Mavromichalaki, A. Papaioannou, C. Plainaki, C. Sarlanis, G. Souvatzoglou, M. Gerontidou, M. Papailiou, E. Eroshenko, A. Belov, V. Yanke, E.O. Flückiger, R. Büttikofer, M. Parisi, M. Storini, K.-L. Klein, N. Fuller, C.T. Steigies, O.M. Rother, B. Heber, R.F. Wimmer-Schweingruber, K. Kudela, I. Strharsky, R. Langer, I. Usoskin, A. Ibragimov, A. Chilingaryan, G. Hovsepyan, A. Reymers, A. Yeghikyan, O. Kryakunova, E. Dryn, N. Nikolayevskiy, L. Dorman, L. Pustil'Nik, Applications and usage of the real-time Neutron Monitor database. *Adv. Space Res.* **47**, 2210–2222 (2011). doi:[10.1016/j.asr.2010.02.019](https://doi.org/10.1016/j.asr.2010.02.019)
- D.J. McComas, R.W. Ebert, H.A. Elliott, B.E. Goldstein, J.T. Gosling, N.A. Schwadron, R.M. Skoug, Weaker solar wind from the polar coronal holes and the whole Sun. *Geophys. Res. Lett.* **35**, 18103 (2008). doi:[10.1029/2008GL034896](https://doi.org/10.1029/2008GL034896)
- D.J. McComas, D. Alexashov, M. Bzowski, H. Fahr, J. Heerikhuisen, V. Izmodenov, M.A. Lee, E. Möbius, N. Pogorelov, N.A. Schwadron, G.P. Zank, The heliosphere's interstellar interaction: no bow shock. *Science* **336**, 1291 (2012). doi:[10.1126/science.1221054](https://doi.org/10.1126/science.1221054)
- D.J. McComas, N. Angold, H.A. Elliott, G. Livadiotis, N.A. Schwadron, R.M. Skoug, C.W. Smith, Weakest solar wind of the space age and the current “mini” solar maximum. *Astrophys. J.* **779**, 2 (2013). doi:[10.1088/0004-637X/779/1/2](https://doi.org/10.1088/0004-637X/779/1/2)
- K.G. McCracken, Heliomagnetic field near Earth, 1428–2005. *J. Geophys. Res.* **112**, 09106 (2007a). doi:[10.1029/2006JA012119](https://doi.org/10.1029/2006JA012119)
- K.G. McCracken, High frequency of occurrence of large solar energetic particle events prior to 1958 and a possible repetition in the near future. *Space Weather* **5**, 7004 (2007b). doi:[10.1029/2006SW000295](https://doi.org/10.1029/2006SW000295)
- K.G. McCracken, G.A.M. Dreschhoff, D.F. Smart, M.A. Shea, A study of the frequency of occurrence of large-fluence solar proton events and the strength of the interplanetary magnetic field. *Sol. Phys.* **224**, 359–372 (2004). doi:[10.1007/s11207-005-5257-2](https://doi.org/10.1007/s11207-005-5257-2)
- K.G. McCracken, G.A.M. Dreschhoff, E.J. Zeller, D.F. Smart, M.A. Shea, Solar cosmic ray events for the period 1561–1994: I. Identification in polar ice, 1561–1950. *J. Geophys. Res.* **106**, 21585–21598 (2001)
- K.G. McCracken, H. Moraal, M.A. Shea, The high-energy impulsive ground-level enhancement. *Astrophys. J.* **761**, 101 (2012). doi:[10.1088/0004-637X/761/2/101](https://doi.org/10.1088/0004-637X/761/2/101)
- F.B. McDonald, Cosmic-ray modulation in the heliosphere a phenomenological study. *Space Sci. Rev.* **83**, 33–50 (1998)
- F.B. McDonald, W.R. Webber, D.V. Reames, Unusual time histories of galactic and anomalous cosmic rays at 1 AU over the deep solar minimum of cycle 23/24. *Geophys. Res. Lett.* **37**(1), 18101 (2010). doi:[10.1029/2010GL044218](https://doi.org/10.1029/2010GL044218)
- R.A. Mewaldt, Cosmic rays in the heliosphere: requirements for future observations. *Space Sci. Rev.* **176**, 365–390 (2013). doi:[10.1007/s11214-012-9922-0](https://doi.org/10.1007/s11214-012-9922-0)
- R.A. Mewaldt, C.M.S. Cohen, J. Giacalone, G.M. Mason, E.E. Cholle, M.I. Desai, D.K. Haggerty, M.D. Looper, R.S. Selesnick, A. Vourlidas, How efficient are coronal mass ejections at accelerating solar energetic particles?, in *AIP Conf. Ser.*, ed. by G. Li, Q. Hu, O. Verkhoglyadova, G.P. Zank, R.P. Lin, J. Luhmann, vol. 1039 (2008), pp. 111–117. doi:[10.1063/1.2982431](https://doi.org/10.1063/1.2982431)

- R.A. Mewaldt, A.J. Davis, K.A. Lave, R.A. Leske, E.C. Stone, M.E. Wiedenbeck, W.R. Binns, E.R. Christian, A.C. Cummings, G.A. de Nolfo, M.H. Israel, A.W. Labrador, T.T. von Roseninge, Record-setting cosmic-ray intensities in 2009 and 2010. *Astrophys. J. Lett.* **723**, 1–6 (2010). doi:[10.1088/2041-8205/723/1/L1](https://doi.org/10.1088/2041-8205/723/1/L1)
- A.L. Mishev, L.G. Kocharov, I.G. Usoskin, Analysis of the ground level enhancement on 17 May 2012 using data from the global neutron monitor network. *J. Geophys. Res.* **119**, 670–679 (2014). doi:[10.1002/2013JA019253](https://doi.org/10.1002/2013JA019253)
- H. Miyahara, K. Masuda, Y. Muraki, H. Furuzawa, H. Menjo, T. Nakamura, Cyclicity of solar activity during the Maunder minimum deduced from radiocarbon content. *Sol. Phys.* **224**, 317–322 (2004). doi:[10.1007/s11207-005-6501-5](https://doi.org/10.1007/s11207-005-6501-5)
- F. Miyake, K. Nagaya, K. Masuda, T. Nakamura, A signature of cosmic-ray increase in ad 774–775 from tree rings in Japan. *Nature* **486**, 240–242 (2012). doi:[10.1038/nature11123](https://doi.org/10.1038/nature11123)
- F. Miyake, K. Masuda, T. Nakamura, Lengths of Schwabe cycles in the seventh and eighth centuries indicated by precise measurement of carbon-14 content in tree rings. *J. Geophys. Res.* **118**, 1–5 (2013). doi:[10.1002/2012JA018320](https://doi.org/10.1002/2012JA018320)
- H. Moraal, P.H. Stoker, Long-term neutron monitor observations and the 2009 cosmic ray maximum. *J. Geophys. Res.* **115**, 12109 (2010). doi:[10.1029/2010JA015413](https://doi.org/10.1029/2010JA015413)
- H. Moraal, A. Belov, J.M. Clem, Design and co-ordination of multi-station international neutron monitor networks. *Space Sci. Rev.* **93**, 285–303 (2000). doi:[10.1023/A:1026504814360](https://doi.org/10.1023/A:1026504814360)
- K. Mursula, T. Hiltula, Bashful ballerina: southward shifted heliospheric current sheet. *Geophys. Res. Lett.* **30**, 2135 (2003). doi:[10.1029/2003GL018201](https://doi.org/10.1029/2003GL018201)
- H.V. Neher, Cosmic-ray particles that changed from 1954 to 1958 to 1965. *J. Geophys. Res.* **72**, 1527 (1967). doi:[10.1029/JZ072i005p01527](https://doi.org/10.1029/JZ072i005p01527)
- H.V. Neher, Cosmic rays at high latitudes and altitudes covering four solar maxima. *J. Geophys. Res.* **76**, 1637–1651 (1971). doi:[10.1029/JA076i007p01637](https://doi.org/10.1029/JA076i007p01637)
- H.W. Newton, *The Face of the Sun* (Penguin Books, Harmondsworth, 1958)
- M.J. Owens, R.J. Forsyth, The heliospheric magnetic field. *Living Rev. Sol. Phys.* **10**, 5 (2013). doi:[10.12942/lrsp-2013-5](https://doi.org/10.12942/lrsp-2013-5)
- M.J. Owens, I. Usoskin, M. Lockwood, Heliospheric modulation of galactic cosmic rays during grand solar minima: past and future variations. *Geophys. Res. Lett.* **39**, 19102 (2012). doi:[10.1029/2012GL053151](https://doi.org/10.1029/2012GL053151)
- E.N. Parker, The passage of energetic charged particles through interplanetary space. *Planet. Space Sci.* **13**, 9–49 (1965)
- M.I. Pishkalo, Reconstruction of the heliospheric current sheet tilts using sunspot numbers. *Sol. Phys.* **233**, 277–290 (2006). doi:[10.1007/s11207-006-1981-5](https://doi.org/10.1007/s11207-006-1981-5)
- N.V. Pogorelov, S.T. Suess, S.N. Borovikov, R.W. Ebert, D.J. McComas, G.P. Zank, Three-dimensional features of the outer heliosphere due to coupling between the interstellar and interplanetary magnetic fields. IV. Solar cycle model based on Ulysses observations. *Astrophys. J.* **772**, 2 (2013). doi:[10.1088/0004-637X/772/1/2](https://doi.org/10.1088/0004-637X/772/1/2)
- M. Potgieter, Solar modulation of cosmic rays. *Living Rev. Sol. Phys.* **10**, 3 (2013). doi:[10.12942/lrsp-2013-3](https://doi.org/10.12942/lrsp-2013-3)
- M.S. Potgieter, R. Strauss, At what rigidity does the solar modulation of galactic cosmic rays begin? in *33rd International Cosmic Ray Conference, Rio de Janeiro, Brazil* (2013), p. 156
- M.S. Potgieter, E.E. Vos, M. Boezio, N. De Simone, V. Di Felice, V. Formato, Modulation of galactic protons in the heliosphere during the unusual solar minimum of 2006 to 2009. *Sol. Phys.* **289**, 391–406 (2014). doi:[10.1007/s11207-013-0324-6](https://doi.org/10.1007/s11207-013-0324-6)
- D.V. Reames, Particle acceleration at the Sun and in the heliosphere. *Space Sci. Rev.* **90**, 413–491 (1999). doi:[10.1023/A:1005105831781](https://doi.org/10.1023/A:1005105831781)
- D.V. Reames, The two sources of solar energetic particles. *Space Sci. Rev.* 53–92 (2013). doi:[10.1007/s11214-013-9958-9](https://doi.org/10.1007/s11214-013-9958-9)
- I.G. Richardson, Geomagnetic activity during the rising phase of solar cycle 24. *J. Space Weather Space Clim.* **3**(26), 260000 (2013). doi:[10.1051/swsc/2013031](https://doi.org/10.1051/swsc/2013031)
- J.D. Richardson, N.A. Schwadron, in *The Limits of Our Solar System*, ed. by M.A. Barucci, H. Boehnhardt, D.P. Cruikshank, A. Morbidelli, R. Dotson (University of Arizona Press, Tucson, 2008), pp. 443–463
- I.G. Richardson, H.V. Cane, E.W. Cliver, Sources of geomagnetic activity during nearly three solar cycles (1972–2000). *J. Geophys. Res.* **107**, 1187 (2002). doi:[10.1029/2001JA000504](https://doi.org/10.1029/2001JA000504)
- M.A. Shea, D.F. Smart, A summary of major solar proton events. *Sol. Phys.* **127**, 297–320 (1990)
- M.A. Shea, D.F. Smart, Significant proton events of solar cycle 22 and a comparison with events of previous solar cycles. *Adv. Space Res.* **14**, 631–638 (1994). doi:[10.1016/0273-1177\(94\)90518-5](https://doi.org/10.1016/0273-1177(94)90518-5)
- M.A. Shea, D.F. Smart, History of solar proton event observations. *Nucl. Phys. B, Proc. Suppl.* **39**, 16–25 (1995)
- M.A. Shea, D.F. Smart, Space weather and the ground-level solar proton events of the 23rd solar cycle. *Space Sci. Rev.* **171**, 161–188 (2012). doi:[10.1007/s11214-012-9923-z](https://doi.org/10.1007/s11214-012-9923-z)

- Y. Shikaze, S. Haino, K. Abe, H. Fuke, T. Hams, K.C. Kim, Y. Makida, S. Matsuda, J.W. Mitchell, A.A. Moiseev, J. Nishimura, M. Nozaki, S. Orito, J.F. Ormes, T. Sanuki, M. Sasaki, E.S. Seo, R.E. Streitmatter, J. Suzuki, K. Tanaka, T. Yamagami, A. Yamamoto, T. Yoshida, K. Yoshimura, Measurements of 0.2–20 GeV/n cosmic-ray proton and helium spectra from 1997 through 2002 with the BESS spectrometer. *Astropart. Phys.* **28**, 154–167 (2007). doi:[10.1016/j.astropartphys.2007.05.001](https://doi.org/10.1016/j.astropartphys.2007.05.001)
- J.A. Simpson, Cosmic radiation neutron intensity monitor, in *Annals of the Int. Geophysical Year IV, Part VII* (Pergamon Press, London, 1958), p. 351
- J.A. Simpson, The cosmic ray nucleonic component: the invention and scientific uses of the Neutron Monitor—(keynote lecture). *Space Sci. Rev.* **93**, 11–32 (2000). doi:[10.1023/A:1026567706183](https://doi.org/10.1023/A:1026567706183)
- D.F. Smart, M.A. Shea, H.E. Spence, L. Kepko, Two groups of extremely large >30 MeV solar proton fluence events. *Adv. Space Res.* **37**, 1734–1740 (2006). doi:[10.1016/j.asr.2005.09.008](https://doi.org/10.1016/j.asr.2005.09.008)
- S.K. Solanki, M. Schüssler, M. Fligge, Evolution of the Sun's large-scale magnetic field since the Maunder minimum. *Nature* **408**, 445–447 (2000)
- S.K. Solanki, I.G. Usoskin, B. Kromer, M. Schüssler, J. Beer, Unusual activity of the Sun during recent decades compared to the previous 11,000 years. *Nature* **431**, 1084–1087 (2004). doi:[10.1038/nature02995](https://doi.org/10.1038/nature02995)
- F. Steinhilber, J.A. Abreu, J. Beer, K.G. McCracken, Interplanetary magnetic field during the past 9300 years inferred from cosmogenic radionuclides. *J. Geophys. Res.* **115**, 01104 (2010). doi:[10.1029/2009JA014193](https://doi.org/10.1029/2009JA014193)
- E.C. Stone, A.C. Cummings, F.B. McDonald, B.C. Heikkila, N. Lal, W.R. Webber, Voyager 1 explores the termination shock region and the heliosheath beyond. *Science* **309**, 2017–2020 (2005). doi:[10.1126/science.1117684](https://doi.org/10.1126/science.1117684)
- E.C. Stone, A.C. Cummings, F.B. McDonald, B.C. Heikkila, N. Lal, W.R. Webber, An asymmetric solar wind termination shock. *Nature* **454**, 71–74 (2008). doi:[10.1038/nature07022](https://doi.org/10.1038/nature07022)
- E.C. Stone, A.C. Cummings, F.B. McDonald, B.C. Heikkila, N. Lal, W.R. Webber, Voyager 1 observes low-energy galactic cosmic rays in a region depleted of heliospheric ions. *Science* **341**, 150–153 (2013). doi:[10.1126/science.1236408](https://doi.org/10.1126/science.1236408)
- Y.I. Stozhkov, N.S. Svirzhevsky, G.A. Bazilevskaya, A.N. Kvashnin, V.S. Makhmutov, A.K. Svirzhevskaya, Long-term (50 years) measurements of cosmic ray fluxes in the atmosphere. *Adv. Space Res.* **44**, 1124–1137 (2009). doi:[10.1016/j.asr.2008.10.038](https://doi.org/10.1016/j.asr.2008.10.038)
- R.D. Strauss, M.S. Potgieter, S.E.S. Ferreira, Modeling ground and space based cosmic ray observations. *Adv. Space Res.* **49**, 392–407 (2012a). doi:[10.1016/j.asr.2011.10.006](https://doi.org/10.1016/j.asr.2011.10.006)
- R.D. Strauss, M.S. Potgieter, I. Büsching, A. Kopp, Modelling heliospheric current sheet drift in stochastic cosmic ray transport models. *Astrophys. Space Sci.* **339**, 223–236 (2012b). doi:[10.1007/s10509-012-1003-z](https://doi.org/10.1007/s10509-012-1003-z)
- L. Svalgaard, E.W. Cliver, Heliospheric magnetic field 1835–2009. *J. Geophys. Res.* **115**, 09111 (2010). doi:[10.1029/2009JA015069](https://doi.org/10.1029/2009JA015069)
- Z. Švestka, Proton flares before 1956. *Bull. Astron. Inst. Czechoslov.* **17**, 262–270 (1966)
- Z. Švestka, P. Simon (eds.), *Catalog of Solar Particle Events 1955–1969*. Astrophysics and Space Science Library, vol. 49 (1975)
- N. Thakur, N. Gopalswamy, H. Xie, P. Makelä, S. Yashiro, S. Akiyama, J.M. Davila, Ground level enhancement in the 2014 January 6 solar energetic particle event. *Astrophys. J. Lett.* **790**, 13 (2014)
- S. Ting, The alpha magnetic spectrometer on the International Space Station. *Nucl. Phys. B, Proc. Suppl.* **243**, 12–24 (2013). doi:[10.1016/j.nuclphysbps.2013.09.028](https://doi.org/10.1016/j.nuclphysbps.2013.09.028)
- A. Tylka, W. Dietrich, A new and comprehensive analysis of proton spectra in ground-level enhanced (GLE) solar particle events, in *31th International Cosmic Ray Conference* (Universal Academy Press, Lodź, 2009)
- A.J. Tylka, M.A. Lee, A model for spectral and compositional variability at high energies in large, gradual solar particle events. *Astrophys. J.* **646**, 1319–1334 (2006). doi:[10.1086/505106](https://doi.org/10.1086/505106)
- A.J. Tylka, C.M.S. Cohen, W.F. Dietrich, M.A. Lee, C.G. MacLennan, R.A. Mewaldt, C.K. Ng, D.V. Reames, Shock geometry, seed populations, and the origin of variable elemental composition at high energies in large gradual solar particle events. *Astrophys. J.* **625**, 474–495 (2005). doi:[10.1086/429384](https://doi.org/10.1086/429384)
- I.G. Usoskin, A history of solar activity over millennia. *Living Rev. Sol. Phys.* **10**, 1 (2013). doi:[10.12942/lrsp-2013-1](https://doi.org/10.12942/lrsp-2013-1)
- I.G. Usoskin, G.A. Kovaltsov, Occurrence of extreme solar particle events: assessment from historical proxy data. *Astrophys. J.* **757**, 92 (2012). doi:[10.1088/0004-637X/757/1/92](https://doi.org/10.1088/0004-637X/757/1/92)
- I.G. Usoskin, H. Kananen, K. Mursula, P. Tanskanen, G.A. Kovaltsov, Correlative study of solar activity and cosmic ray intensity. *J. Geophys. Res.* **103**, 9567–9574 (1998). doi:[10.1029/97JA03782](https://doi.org/10.1029/97JA03782)
- I.G. Usoskin, K. Mursula, G.A. Kovaltsov, Heliospheric modulation of cosmic rays and solar activity during the Maunder minimum. *J. Geophys. Res.* **106**, 16039–16046 (2001). doi:[10.1029/2000JA000105](https://doi.org/10.1029/2000JA000105)

- I.G. Usoskin, K. Alanko-Huotari, G.A. Kovaltsov, K. Mursula, Heliospheric modulation of cosmic rays: monthly reconstruction for 1951–2004. *J. Geophys. Res.* **110** (2005). doi:[10.1029/2005JA011250](https://doi.org/10.1029/2005JA011250)
- I.G. Usoskin, S.K. Solanki, G.A. Kovaltsov, Grand minima and maxima of solar activity: new observational constraints. *Astron. Astrophys.* **471**, 301–309 (2007). doi:[10.1051/0004-6361/20077704](https://doi.org/10.1051/0004-6361/20077704)
- I.G. Usoskin, G.A. Bazilevskaya, G.A. Kovaltsov, Solar modulation parameter for cosmic rays since 1936 reconstructed from ground-based neutron monitors and ionization chambers. *J. Geophys. Res.* **116**, 02104 (2011). doi:[10.1029/2010JA016105](https://doi.org/10.1029/2010JA016105)
- I.G. Usoskin, B. Kromer, F. Ludlow, J. Beer, M. Friedrich, G.A. Kovaltsov, S.K. Solanki, L. Wacker, The AD775 cosmic event revisited: the Sun is to blame. *Astron. Astrophys.* **552**, 3 (2013). doi:[10.1051/0004-6361/201321080](https://doi.org/10.1051/0004-6361/201321080)
- I.G. Usoskin, G. Hulot, Y. Gallet, R. Roth, A. Licht, F. Joos, G.A. Kovaltsov, E. Thébault, A. Khokhlov, Evidence for distinct modes of solar activity. *Astron. Astrophys.* **562**, 10 (2014). doi:[10.1051/0004-6361/201423391](https://doi.org/10.1051/0004-6361/201423391)
- L.E.A. Vieira, S.K. Solanki, Evolution of the solar magnetic flux on time scales of years to millennia. *Astron. Astrophys.* **509**, 100 (2010). doi:[10.1051/0004-6361/200913276](https://doi.org/10.1051/0004-6361/200913276)
- K.P. Wenzel, R.G. Marsden, D.E. Page, E.J. Smith, The ULYSSES mission. *Astron. Astrophys. Suppl. Ser.* **92**, 207–219 (1992)
- E.W. Wolff, M. Bigler, M.A.J. Curran, J.E. Dibb, M.M. Frey, M. Legrand, J.R. McConnell, The Carrington event not observed in most ice core nitrate records. *Geophys. Res. Lett.* **39**, 08503 (2012). doi:[10.1029/2012GL051603](https://doi.org/10.1029/2012GL051603)
- B. Zieger, M. Opher, N.A. Schwadron, D.J. McComas, G. Tóth, A slow bow shock ahead of the heliosphere. *Geophys. Res. Lett.* **40**, 2923–2928 (2013). doi:[10.1002/grl.50576](https://doi.org/10.1002/grl.50576)